HHS Public Access

Author manuscript

Dev Biol. Author manuscript; available in PMC 2015 April 30.

Published in final edited form as:

Dev Biol. 2013 August 1; 380(1): 111–124. doi:10.1016/j.ydbio.2013.03.011.

Polycomb silencing of the *Drosophila 4E-BP* gene regulates imaginal disc cell growth

Heather Mason-Suares[1], **Feng Tie**[1], **Christopher Yan**[1,2], and **Peter J. Harte**[1]

[1]Department of Genetics, Case Western Reserve University, School of Medicine, 10900 Euclid Avenue, Cleveland, OH 44106, USA

[2]Department of Molecular Genetics and Microbiology, Duke University Medical Center, Research Drive, Durham, NC 27710

Abstract

Polycomb group (PcG) proteins are best known for their role in maintaining stable, mitotically heritable silencing of the homeotic (HOX) genes during development. In addition to loss of homeotic gene silencing, some PcG mutants also have small imaginal discs. These include mutations in *E(z)*, *Su(z)12*, *esc* and *escl*, which encode Polycomb Repressive Complex 2 (PRC2) subunits. The cause of this phenotype is not known, but the human homologs of PRC2 subunits have been shown to play a role in cell proliferation, are over-expressed in many tumors, and appear to be required for tumor proliferation. Here we show that the small imaginal disc phenotype arises, at least in part, from a cell growth defect. In homozygous *E(z)* mutants, imaginal disc cells are smaller than cells in normally proliferating discs. We show that the *Thor* gene, which encodes eIF4E-Binding Protein (4E-BP), the evolutionarily conserved inhibitor of cap-dependent translation and potent inhibitor of cell growth, is involved in the development of this phenotype. The *Thor* promoter region contains DNA binding motifs for transcription factors found in well-characterized Polycomb Response Elements (PREs), including PHO/PHOL, GAGA Factor, and others, suggesting that *Thor* may be a direct target of Polycomb silencing. We present chromatin immunoprecipitation evidence that PcG proteins are bound to the *Thor* 5' region in vivo. The *Thor* gene is normally repressed in imaginal discs, but *Thor* mRNA and 4E-BP protein levels are elevated in imaginal discs of PRC2 subunit mutant larvae. Deletion of the *Thor* gene in *E(z)* mutants partially restores imaginal disc size toward wild-type and results in an increase in the fraction of larvae that pupariate. These results thus suggest that PcG proteins can directly modulate cell growth in *Drosophila*, in part by regulating *Thor* expression.

Keywords

Polycomb silencing; *Thor* gene; 4E-binding protein; cell growth

Corresponding Author: Peter J. Harte, Department of Genetics, Case Western Reserve University School of, Medicine, 2109 Adelbert Road, Cleveland, OH, 44106. telephone: (216) 368-6417 fax: (216) 368-3432 pjh3@case.edu.

Introduction

Polycomb group (PcG) genes are best known for their role in stable, mitotically heritable silencing of the *Drosophila* homeotic genes in cells outside of their normal, spatially restricted expression domains (Campbell et al., 1995; Jurgens et al., 1984; McKeon and Brock, 1991; Simon et al., 1992). More recently, investigations of PcG genes in *Drosophila*, mice, and human cells have implicated them in a growing number of biological processes, including stem cell maintenance and differentiation (Lee et al., 2006; Pasini et al., 2007), mammalian X-chromosome inactivation (Fang et al., 2004; Mak et al., 2002; Wang et al., 2001; Zhao et al., 2008), tissue regeneration and wound healing (Maurange et al., 2006; Shaw and Martin, 2009), inflammation (DeSanta et al., 2007), DNA repair and apoptosis (Holmes et al., 2006), regulation of cell cycle exit and cell senescence (Oktaba et al., 2008; Sparmann and van Lohuizen, 2006) and tumorigenesis (Simon and Lange, 2008). Consistent with this, recent genome-wide mapping of sites bound by PcG proteins in *Drosophila* and human cells have identified hundreds of new Polycomb target genes (Boyer et al., 2006; Bracken et al., 2006; Lee et al., 2006; Schwartz et al., 2006). Many of these encode transcription factors and signaling pathway components, suggesting PcG proteins also indirectly affect the expression of many more genes (Schwartz et al., 2006).

Polycomb silencing requires collaboration among several multi-protein complexes on chromatin, including Polycomb Repressive Complexes 1 and 2 (PRC1 and PRC2) (Klymenko et al., 2006; Mohd-Sarip et al., 2005; Mohd-Sarip et al., 2006; Oktaba et al., 2008; Schwartz and Pirrotta, 2007). PRC2-specific subunits include the PcG proteins E(Z), SU(Z)12, ESC (or its closely related paralog, ESCL), and PCL (Cao et al., 2002; Czermin et al., 2002; Kurzhals et al., 2008; Müller et al., 2002; Nekrasov et al., 2005; Ohno et al., 2008; Schwartz and Pirrotta, 2008; Tie et al., 2003), as well as the CAF-1 p55 subunit (Schmitges et. al., 2011). The PRC2 catalytic subunit, E(Z), specifically mono-, di- and tri-methylates histone H3 on lysine 27, the trimethyl-H3K27 mark (H3K27me3) being required for Polycomb silencing (Cao et al., 2002; Czermin et al., 2002; Ketel et al., 2005; Nekrasov et al., 2005). This activity requires the other non-catalytic PRC2 subunits, including the histone H3 binding subunit ESC or its paralog ESCL (Czermin et al., 2002; Kurzhals et al., 2008; Pasini et al., 2007; Tie et al., 2007; Ohno et al., 2008; Wang et al., 2006). The PRC1 complex binds specifically to nucleosomes containing H3K27me3, via the chromodomain of its PC subunit. The PRC1 SCE/RING subunit monoubiquitylates histone H2A on lysine 119, another modification required for silencing of some Polycomb regulated genes (Gutiérrez et al., 2012; Wang et al., 2004). Recent genome-wide mapping studies have shown that H3K27me3 and PcG proteins are distributed over broad regions that include promoters, flanking regulatory regions and transcribed regions of Polycomb regulated genes, with the promoter suspected to be the key site of action of PRC1 (Bloyer et al., 2003; Enderle et al., 2011; Oktaba et al., 2008; Park et al., 2012; Schuettengruber et al., 2009; Schwartz et al., 2010). Recent biochemical evidence indicates that the recruitment of PRC1 to promoters can inhibit assembly of transcription preinitiation complexes (Lehmann et al., 2012).

PRC1 and PRC2 are recruited to Polycomb target genes through a variety of mechanisms, including interactions with sequence-specific DNA binding proteins that bind directly to cis-acting Polycomb Response Elements (PREs) (Chan et al., 1994; Christen and Bienz, 1994; Schwartz and Pirrotta, 2007; Simon et al., 1993). One of the key recruiters found in many well-characterized PREs is the DNA binding protein PHO (Brown et al., 1998), along with its closely related paralog PHO-like (PHOL) (Brown et al., 2003), both of which are homologs of mammalian YY1. PHO is present in the Pho-RC complex, which appears to be required for Polycomb silencing (Klymenko et al., 2006). Binding sites for GAGA Factor (GAF) are also present in well characterized PREs. GAF has been implicated in Polycomb silencing (Hagstrom et al., 1997; Hodgson et al., 2001), recruiting PRC1 and facilitating binding of PHO to adjacent sites on chromatin (Mahmoudi et al., 2003). Once recruited, subsequent regulated interactions of PRC2 and PRC1 with promoter chromatin and surrounding regions lead to local deposition of H3K27me3 and transcriptional silencing. We do not yet have a detailed understanding of the mechanism of Polycomb silencing, but there may be several different modes of action of Polycomb complexes, which may depend on different types of PREs. The PREs in the homeotic genes, which can act over long distances and promote complete transcriptional silencing of their target genes, are examples of one type (Muller and Kassis, 2006). Examples of a second type, which act only at short range and function more like governors or rheostats than silencers by limiting or down-regulating rather than silencing the level of transcription, are found in the adjacent paralogous PcG genes *ph-p* and *ph-d* genes (Bloyer et al., 2003), as well as *Psc* and *Su(z)2* (Park et al., 2012), and the *CycB* gene (Oktaba et al., 2008).

Before *E(z)* was recognized as a PcG gene (Jones and Gelbart, 1990; Phillips and Shearn, 1990), Shearn and colleagues (1978) identified a loss-of-function allele (originally *l(3)1902 or* pco^{1902}, now $E(z)^{5}$) in a screen for late larval/prepupal lethals that cause imaginal disc abnormalities. Larvae homozygous or hemizygous for this mutation and for other subsequently identified alleles have small imaginal discs that never reach mature size. Dorsal discs are more severely affected than ventral discs (Phillips and Shearn, 1990). Mutant larvae die either at the end of third instar or after undergoing pupariation, but do not progress to the pupal stage, the definitive start of metamorphosis whose onset is marked by eversion of the imaginal head. Their small imaginal discs are not due to cell death, as indicated by their failure to take up acridine orange (LaJeunesse and Shearn, 1996). They are viable through several rounds of transplantation and *in vivo* culture in adult female abdomens, but they remain incompetent to differentiate when transplanted into wild type larval hosts that subsequently undergo metamorphosis, indicating that the *E(z)* small disc mutant phenotype is disc-autonomous (Shearn et al., 1978). Other PRC2 subunit mutants exhibit the same phenotype. Homozygous *esc, escl* double mutants also have small imaginal discs and fail to pupate (Kurzhals et al., 2008). Additionally, *pho, phol* double mutants exhibit a similar phenotype, consistent with the proposed role of PHO and PHOL in recruiting PRC2 to chromatin (Brown et al., 2003).

The survival of *E(z), Su(z)12* and *esc, escl* double mutants through embryogenesis is due to maternal rescue. *esc, escl* double mutants die at the end of third instar (Kurzhals et al., 2008). *Su(z)12* mutants can die as late as second instar (Birve et al., 2001). Mutant embryos

lacking functional E(Z), SU(Z)12 or ESC of maternal origin are late embryonic lethal and exhibit characteristic Polycomb phenotypes, i.e., transformation of all segments to eighth abdominal segment identity (Birve et al., 2001; Jones and Gelbart, 1990; Phillips and Shearn, 1990; Struhl, 1983). As a result of maternal rescue, homozygous *E(z)* mutants hatch from the egg and initiate imaginal disc proliferation, which subsequently ceases, presumably when the E(Z) of maternal origin is exhausted.

The causes of the small imaginal disc phenotype of PRC2 subunit mutants are unknown. Here we report that it is associated with a cell growth defect and is due in part to derepression of the *Thor* gene, which encodes the sole *Drosophila* homolog of the eIF4E-Binding Protein (4E-BP), the global inhibitor of cap-dependent mRNA translation. We show that the *Thor* gene is regulated by PcG proteins. In PRC2 subunit mutants the *Thor* gene is derepressed in imaginal discs, where it is normally silenced (Bernal and Kimbrell, 2000; Rodriguez et al., 1996; Teleman et al., 2005), presumably to promote their rapid proliferation during the larval period. Genetic removal of the *Thor* gene in *E(z)* mutants partially rescues their small imaginal disc phenotype and increases their frequency of pupariation, but not their failure to initiate metamorphosis. These data suggest that derepression *of Thor* in imaginal discs of PRC2 subunit mutants is at least partly responsible for their cell proliferation defects through its inhibitory effect on cap-dependent translation and cell growth.

Materials and Methods

Fly Strains, Cell Lines, and Reagents

Drosophila S2 cells were obtained from the *Drosophila* Genomics Resource Center (Bloomington, IN, stock 6). All flies were grown at 25°C on 1% yeast standard media. Fly stocks were obtained from Bloomington Stock Center (Bloomington, IN), except $Thor^{\Delta 1034–2617}$, which is a deletion of the entire 4E-BP coding sequence (Tettweiler et al., 2005) (referred to hereafter out as $Thor^{1034}$) and was obtained from Paul Lasko. $E(z)^{5}$ was obtained from Allen Shearn and $E(z)^{63}$ was obtained from Richard Jones. $E(z)^{63}$ (M1I) is an apparent protein-null mutation (Carrington and Jones, 1996). $E(z)^{5}$ was induced by N-methyl-N'-nitro-N-nitrosoguanidine (Shearn et al., 1978) and was found to be a genetic null allele (LaJeunesse and Shearn, 1996). $E(z)^{731}$ (W638X) is predicted to truncate the E(Z) protein within the SET domain and would produce a catalytically dead protein, but has been reported to produce no detectable protein (Müller et al., 2002). *Df(3L)lxd6* is a deletion of the entire *E(z)* gene and surrounding genes. esc^{6} is a null point mutation causing a failure to splice the first intron (Gutjahr et al., 1995). $escl^{1}$ is a homozygous viable, strong hypomorphic allele (Kurzhals et al., 2008). $Su(z)12^{5}$ *is* a hypomorph and $Su(z)12^{3}$ (W298X) is an apparent null allele (Birve et al., 2001). $Thor^{2}$ is a reported to be a null allele (Bernal and Kimbrell, 2000; Bernal et al., 2004). The 4E-BP 1898 antibody was generously provided by Paul Lasko (Miron et al., 2001). PcG protein antibodies (rabbit anti-E(Z), rabbit anti-ESC, and guinea pig anti-SU(Z)12) have been described previously (Tie et al., 1998; Tie et al., 2001; Tie et al., 2005). Monoclonal anti-β tubulin antibody was obtained from the Developmental Studies Hybridoma Bank (Iowa City, Iowa, stock E7).

Identification of the DNA binding protein motifs

The *Thor* gene (AE014134) was initially inspected visually for PHO, GAF, Sp1/KLF, DSP1, and Zeste binding sites using consensus sites identified in Supplementary Table 1 and also by using the jPREdictor program version 1.23 (http://bibiserv.techfak.uni-bielefeld.de/jpredictor/) as described in Fiedler and Rehmsmeier, 2006 and Ringrose et al., 2003. The extended gene region, taken from Flybase.org, of the *Thor* gene of *melanogaster* (FBgn0261560; 2L: 3476434…3481612), *simulans* (FBgn0067508; 2L:3429948…3434708), *sechellia* (FBgn0166088; scaffold_129:38579…43338), *yakuba* (FBgn0067434; 2L:3464181…8968), *erecta* (FBgn0117077; scaffold_4929:3511402..3516160), *pseudoobscura* (FBgn00813524_group3:complement_ (5269802.. 5274438), *perimilis* (FBgn0156257; scaffold_1:complement (6760558..6765191), *willistoni* (FBgn0220434 scaffold f2_1100000004945:427516..432091), *mojavensis* (FBgn0137757 scaffold_6500:complement (2553576..2558137), *virilis* (FBgn0204414; scaffold_12963:8766725…8771312), and *grimshawi* (FBgn0117695; scaffold_15252: complement (13016175..13020746) were scanned for frequencies of paired (double and MultiMotifs) motifs. The motif sequences are listed in Supplementary Table 1. The motif weighs are as described by Fiedler and Rehmsmeier, 2006 and Ringrose et al., 2003 (Supplementary Fig. 1). The jPREdictor score were determined by scanning a window width of 500 that is moved over the input sequence in steps of 10 bp (Fiedler and Rehmsmeier, 2006). The numerical jPREdictor score of each window was plotted in Graph Pad Prism 4 and the highest score for each species was listed in Table 1. To get a significance estimation of scores, we scanned a random sequence of equal size and nucleotide distribution of each tested sequence and used the empirical score distribution to define score thresholds for E values of 0.05. The E value is defined as the number of times you expect to find a region with a score equal to or higher in a sequence of the corresponding length and nucleotide composition, for example a score with an E value of 0.05 would be expected to occur only once by chance in twenty sample sequences (Ringrose et al., 2003).

Chromatin Immunoprecipitation (ChIP)

ChIP was conducted with the PC, ESC, SU(Z)12, and E(Z) antibodies as described previously (Tie et al., 2007). PCR and qPCR reactions amplified a 115 bp fragment of the *Thor* promoter (Fig. 3C). Primer sequences are available upon request.

To ensure that PCR amplification was in the linear range, each reaction was initially set up at different MgCl2 concentrations and varying amplification cycle number. PCR reactions where amplified for 15,20, 25, 27, 30, and 32 cycles to determine the optimal number of cycles. Furthermore, different $MgCl_2$ concentrations of 1, 1.5, 2, 3, 5 μM were tested. Reactions were carried out for 27 cycles in a buffer concentration of 1.5 μM $MgCl_2$. Assays were run in triplicate.

Real time qPCR reactions were run on the BioRad Chromo 4 using the Platinum SYBR Green QPCR master mix (Invitrogen catalog # 11733-046). The assay was done in triplicate and three biological replicates of each sample were assayed for a total of nine reactions.

ChIP followed by microarray analysis (ChIP-chip) was conducted in cultured S2 cells as previously described (Tie et al., 2009). The anti-PC antibody was raised in rabbits against full length PC and its specificity confirmed by western after *Pc* RNAi knockdown in S2 cells (Fig. 3F). EZ View Red anti-HA affinity gel (Sigma, catalog # E6779) was used to immunoprecipitate chromatin bound by HA-tagged PC from a stable S2 cell line expressing HA-PC from the *Act5C* promoter or as a negative control from normal S2 cells. Cy3 and Cy5 random primer labeling of input and ChIP-enriched samples was carried out using a CGH Labeling Kit for Oligo Arrays (Enzo, 42671). Labeled ChIP-enriched and input samples were co-hybridized to *Drosophila melanogaster* tiling microarrays (NimbleGen, DM_5_Catolog_tiling_HX1). NimbleScan software and Integrated Genome Browser (1.5 GB; Affymetrix) were used for analysis.

Cell culture and double-stranded RNA interference (RNAi)

Drosophila S2 cells were cultured at 27°C in Schneider's medium (Invitrogen, catalog # 11720034) supplemented with 10% fetal bovine serum (FBS) (Invitrogen, catalog #16000-036). Double-stranded RNAs (dsRNAs) were generated in vitro, and RNAi was performed as previously described (Tie et al., 2007). For the RNAi, S2 cells were treated with 15 μg/mL of dsRNA for 7 days, with fresh dsRNA and media added every other day. To deplete *esc*, a 490 bp dsRNA extending from the start codon, was used. To deplete *escl*, a 619 bp dsRNA extending from the start codon of *escl* was used. To deplete *E(z), Su(z)12, and Pc*, a 700 bp dsRNA for each, extending from the start codon, was used. A GFP dsRNA was used as a negative control. Whole cell extracts were prepared in 40 mM Tris (pH 7.5), 8.0 M urea and analyzed by Western blot. Alternatively, total RNA was extracted using Trizol reagent according to the manufacturer's protocol (Invitrogen, catalog #15596-018).

Real Time qRT-PCR Analysis

Total RNA was extracted from RNAi treated S2 cells using the Trizol reagent according to the manufacturer's protocol (Invitrogen, catalog #15596-018) or third instar larval imaginal disc and brain tissue using the Zymed Mini RNA Isolation I Kit, catalog # R1005. cDNA was generated using total RNA from each sample, SuperScript III Reverse Transcriptase (Invitrogen, catalog # 18080044), and random primers (Promega, catalog # C1181). The resulting cDNA was used as template for real time qRT-PCR (quantitative reverse transcriptase-polymerase chain reaction) with intron-spanning primers for *Thor* or *RpS12*. Real time qRT-PCR reactions were run on the BioRad Chromo 4 using the Platinum SYBR Green QPCR master mix (Invitrogen catalog # 11733-046). All assays were done in triplicate and three biological replicates of each sample were assayed for a total of nine reactions for each genotype. RNA expression levels were normalized to *RpS12* expression. T-tests were run on Graph Pad Prism 4.

Imaginal Disc Immunochemistry and Area Measurements

Late third instar larvae were dissected, fixed in 4% formaldehyde in PBST for 20 minutes at room temperature, and then washed in PBST. Imaginal discs were either mounted in Vectashield mounting media (Vector, catalog # H-1000) and photographed in brightfield (10X) on a Leica M16 microscope or used for antibody staining. For disc area

measurements, discs were photographed on a Leica DM6000 microscope. Photographed discs were outlined and measured using Velocity 4.4 software (Improvision). T-tests were run on Graph Pad Prism 4 (La Jolla, CA). For wing disc cell area measurements, fixed discs were blocked with 3% BSA in PBS, incubated in Oregon Green 488 phalloidin (Invitrogen, catalog #O7466) in 1% BSA in PBS for thirty minutes at room temperature and then washed three times in 1% PBST. The discs were photographed on a Leica DM6000 microscope. Photographed wing disc cells were outlined and cell area was measured using Velocity 4.4 software (Improvision). T-tests were run on Graph Pad Prism 4. For antibody staining, fixed discs were blocked with 3% BSA in PBST, incubated in the d4E-BP 1898 antibody in 3% BSA in PBST overnight at 4°C, washed, and then incubated with Alexa Fluor 488 goat anti-rabbit antibody (Invitrogen, catalog # A-11034) for 2 hours at room-temperature. Discs were mounted in Vectashield mounting medium with DAPI (Vector, catalog # H-1200) and images were obtained using a Bio-Rad MRC-600 confocal imaging system.

Western Blot

Imaginal discs and brain tissue were dissected from wandering third instar larvae. Tissue from 20 larvae were homogenized in 40 μL RIPA buffer (50 mM Tris, 150 mM NaCl, 0.1% SDS, 0.5% Na Deoxycholate, Triton X-100,) and incubated on ice for 20 minutes. Lysates were run on 15% sodium dodecyl sulfate (SDS)-polyacrylamide gel electrophoresis (PAGE) and transferred to a 0.2 μm nitrocellulose membrane (Whatman, catalog # 926–31092). The membrane was blocked with 10% nonfat dry milk in PBST for 1 hour and then incubated with 4E-BP 1898 antibody (1:1000 dilution) over-night at 4°C. The membrane was subsequently incubated with donkey anti-rabbit antibody (1:10,000 dilution) (GE Healthcare, catalog # NA934-100UL) for 1 hour at room temperature. All antibody incubations were followed by multiple washes with PBST. SuperSignal West Dura substrate (Thermo Scientific, catalog # 34075) (1:10 dilution) was used for visualization of bound antibody.

Results

Homozygous PRC2 mutants exhibit cell growth and proliferation defects

Shearn and colleagues found that the small imaginal disc phenotype of homozygous *E(z)* mutants was not due to increased apoptosis (LaJeunesse and Shearn, 1996; Phillips and Shearn, 1990). Consistent with this, the neuroblasts in the larval protocerebral lobes of *E(z)* and other PcG mutants exhibit a very low mitotic index (Bello et al., 2007; Gatti and Baker, 1989; Philips and Shearn, 1990) suggesting a cell proliferation defect. We examined the small wing discs *of E(z)* mutants more closely, and found that the area of the wing disc cells was also reduced by 75% compared to wild type controls of the same stage (Fig. 1). This suggests that the small imaginal disc phenotype is due, at least in part, to a defect in imaginal cell growth, which may also contribute to the observed arrest of proliferation.

Identification of *Thor* as a potential direct target of PcG proteins

To determine whether the small size *of E(z)* mutant imaginal disc cells might be caused by a gene that is directly regulated by Polycomb silencing, we searched the sequences of genes that encode regulators of cell growth, including the Insulin and TOR signaling pathways, for

binding motifs (Supplementary Table 1) of DNA binding proteins found in well-characterized Polycomb Response Elements (PREs) (Brown and Kassis, 2010; Busturia et al., 2001; Dejardin et al., 2005; Horard et al., 2000; Ringrose et al., 2003; Strutt et al., 1997). We identified the *Thor* gene as a potential target of Polycomb silencing. As shown in Fig. 2A, binding motifs for Pleiohomeotic (PHO), GAGA factor (GAF) or Pipsqeak (PSQ), Sp1/KLF, Dorsal switch protein 1 (DSP1), and Zeste are present in the vicinity of the *Thor* promoter and 5' UTR. In addition, we analyzed the *Thor* gene with the most recent version of the jPREdictor program (version 1.23) (Fiedler and Rehmsmeier, 2006; Ringrose et al., 2003) to identify sequence motifs found in well-characterized PREs. The analysis using jPREdictor identified a peak in the *Thor* promoter region with a significant jPREdictor score of 82.11 corresponding to the location of the previously identified binding sites (Fig. 2A).

Evolutionary conservation of DNA binding motifs in distantly related species can provide strong evidence that the conserved motifs may be functionally important. Analyses of PRE conservation within *Drosophila* species have indicated that while no single binding motif can be used to identify all PREs and while the presence of key binding sites is often conserved, the precise number, order and location of different binding sites is relatively poorly conserved (Dellino et al., 2002; Hauenschild et al., 2008). Alignment of the sequence of the *D. melanogaster Thor* gene with those of other *Drosophila* species that diverged up to 8 million years ago (MYA) revealed that some of the binding motifs present in the *D. melanogaster Thor* gene have been evolutionarily conserved in these other *Drosophila* species (Fig. 2B). There were some differences in the number of GAF/PSQ binding sites and a loss of one putative PHO/PHOL binding site in the other species. However, it was previously shown that PHO also binds *in vitro* to specific DNA fragments that do not contain any of the known PHO binding motifs (Cunningham et al., 2010) suggesting there may be undetected PHO binding sites that would be missed in this study. Overall, the *Thor* promoter has a conserved motif order and location for at least 8 million years.

To determine if more divergent *Drosophila* species also have these DNA binding motifs, we analyzed an extended *Thor* gene region for each of the ten other sequenced species using the jPREdictor software, which predicted a significant peak (score) in the *Thor* promoter regions of *melanogaster*, *simulans*, *sechellia*, *yakuba*, *willistoni*, *virilis*, and *grimshawi* (Table 1, Fig. 3A), the latter species diverging from *D. melanogaster* at least 40 MYA. However, jPREdictor did not predict a peak in *erecta*, *pseudoobscura*, *perimilis*, *and mojavensis* (Table 1). The lack of a predicted peak in *erecta* was not expected as the *Thor* sequence is highly conserved when compared to *melanogaster* (Fig. 2B). The highest weighted motif utilized in the jPREdictor program is the PHO motif (Supplementary Fig. 1), and some of the PHO motifs are missing or degenerate in the *erecta* sequence (Fig. 2B), suggesting that this is why jPREdictor failed to predict a significant score for *erecta* and likely the other species with an insignificant score (Table 1). However, some sequences that are bound by PcG proteins *in vivo* were not predicted to be PcG targets by the jPREdictor program (Cunningham et al., 2010).

These data suggest that DNA binding motifs in the vicinity of the *Thor* promoter may recruit PcG proteins. The presence of a cluster of such sites in the vicinity of the promoter is a hallmark of regulation by PcG proteins (Oktaba et al., 2008; Ringrose et al., 2003; Enderle

et al., 2011). PcG proteins are also found within the transcribed regions of many recently identified putative Polycomb regulated genes (Chanas et al., 2005; Cunningham et al., 2010; Martinez et al., 2006; Oktaba et al., 2008; Park et al., 2012).

The *Thor* gene is bound by PcG proteins

To determine whether PcG proteins are bound to the *Thor* promoter, we performed chromatin immunoprecipitation (ChIP) assays with chromatin isolated from S2 cells using antibodies against the PcG proteins PC, E(Z), ESC, and SU(Z)12. The *Thor* gene is expressed in these cells (Chintapalli et al., 2007). As shown in Fig. 3D, E(Z), SU(Z)12, and PC were bound in the vicinity of the *Thor* promoter in S2 cells. The lower ESC signal could reflect binding of an alternative ESCL-containing PRC2 complex also present in S2 cells (Kurzhals et al., 2008). Hybridization of the DNA recovered from ChIP with an anti-PC antibody to *Drosophila* whole genome tiling arrays (ChIP-chip) revealed a single broad peak of PC binding over the promoter region of *Thor* (Fig. 3B). Similar results were found using an anti-HA antibody that recognizes an HA-tagged PC expressed from the *actin 5C* promoter in a stably transfected S2 cell line (that also contains endogenous PC) (Fig. 3B). In both cases the PC peak was among the top 1% of the PC signals genome-wide. The lower peak seen in the HA-tagged PC ChIP is likely due to competition between endogenous PC and HA-tagged PC for binding to the *Thor* promoter (Fig. 3B). For comparison, the ChIP-chip profiles for the Bithorax Complex obtained from the same chromatin preparations with the anti-PC and anti-HA antibodies are very similar to each other and to previously published profiles (Supplementary Fig. 2).

Analysis of data from a recent study using ChIP followed by next generation sequencing (ChIP-seq) (Enderle et al., 2011) revealed that PC, PH and also TRX are bound in the *Thor* promoter region (Supplementary Fig. 3). TRX has been shown to be constitutively bound to virtually all known and presumed PREs (Schwartz et al., 2010). H3K4me3, a highly predictive mark of active genes, is also enriched there (Supplementary Fig. 3), consistent with the transcriptionally active status of *Thor* in S2 cells (Supplementary Fig. 3). Together with the strong TRX peak, this strongly suggests that *Thor* is directly regulated by PcGs. A recent ChIP-seq study from whole third instar larval chromatin also shows binding of SU(Z)12 to the *Thor* gene (Hertz et al., 2011). Similar ChIP-chip data from 4–12 hr embryos (Schuettengruber et al., 2009) shows that the PHO paralog PHOL is also bound at the *Thor* promoter region (Supplementary Fig. 4). Interestingly, while PHO and PHOL appear to recognize the same DNA sequences and are thought to be at least partially functionally redundant, Schuettengruber et al., (2009) reported that PHO was enriched at silent PcG regulated genes, while PHOL was enriched at active PcG regulated genes.

RNAi knockdown of PcG proteins in S2 cells upregulates *Thor* expression

To determine whether the binding of PcG proteins to the *Thor* promoter reflects their function in silencing or down-regulating its expression, we used RNAi knockdown to deplete either PC, E(Z), SU(Z)12, ESC, or both ESC and ESCL in S2 cells. While *4E-BP* mRNA was readily detected in untreated control S2 cells (Chintapalli et al., 2007), its level was elevated more than 2-fold after depletion of PC, E(Z), SU(Z)12, or both ESCL and ESC, as determined by real time quantitative reverse transcriptase-PCR (qRT-PCR) (Fig.

3E). Not surprisingly, knockdown of ESC alone did not result in a significant increase in *4E-BP* mRNA, since ESCL can substitute for ESC in PRC2 in S2 cells (Kurzhals et al., 2008). These data, together with the ChIP results, suggest that PcG proteins directly target *Thor* in S2 cells, but do not completely silence its expression. Instead, they appear to function more like *a* governor to modulate its levels downward, similar to what has been observed for the Polycomb target genes *CycB* (Oktaba et al., 2008), *ph-d* and *ph-p* (Bloyer et al., 2003) and *Psc* and *Su(z)2* (Park et al., 2012). Interestingly, *Thor* was also among the genes whose mRNA levels were found to be elevated after RNAi knockdown of *Pc* in embryos, assayed by microarray-based transcript profiling (Goodliffe et al., 2005). Its level was elevated 1.74 fold, similar to what we see in S2 cells, which are of embryonic origin.

The *Thor* gene is derepressed in imaginal discs in PcG mutants

During the larval stage, *4E-BP* RNA is readily detected in the fat body, salivary glands, midgut, and body wall (Bernal and Kimbrell, 2000; Chintapalli et al., 2007; Rodriguez et al., 1996; Teleman et al., 2005), but is undetectable in imaginal discs by *in situ* hybridization (Bernal and Kimbrell, 2000) and by qRT-PCR (Teleman et al., 2005). To determine whether PcG proteins are bound to the *Thor* promoter in imaginal discs, we performed ChIP-PCR and qPCR assays on chromatin isolated from dissected imaginal discs using antibodies against the PcG proteins PC and E(Z). Both PC and E(Z) were bound to the *Thor* promoter region (Fig. 4A, 4B).

To determine whether the *Thor* gene is derepressed in imaginal discs of PcG mutants, we measured *4E-BP* mRNA levels by real time qRT-PCR in imaginal discs dissected from wild type and *E(z)* mutant third instar larva. Some attached larval CNS tissue, which has very low 4E-BP expression (Chintapali et al., 2007), was dissected along with the imaginal discs. Therefore, the Oregon-R (OR) wild-type control does have low levels of *4E-BP* expression (Fig. 4F). Imaginal discs from the $E(z)^{63}/E(z)^{5}$ heteroallelic combination exhibited a greater than four fold increase in *4E-BP* RNA compared to wild type controls flies and sibling $E(z)^{63}$/TM6B, which have wild-type sized imaginal discs (Fig. 4F). These results are consistent with the *Thor* gene being subject to Polycomb silencing in imaginal discs.

We also examined 4E-BP protein expression in wing imaginal discs of wild type and PRC2 mutant third instar larvae, including esc^{6} $escl^{1}$ double mutants, heteroallelic $Su(z)12^{5}/Su(z)12^{3}$, $E(z)^{63}/Df(3L)lxd6$, and $E(z)^{63}/E(z)^{5}$ mutants, all of which have small imaginal discs. Immuno-fluorescent staining with an anti-4E-BP antibody (Miron et al., 2001) detected no 4E-BP protein in wild type discs, while a substantial signal is seen in wing discs from each of the PRC2 mutants (Fig. 4C). Interestingly, we also observed an increase in the amount of 4E-BP protein in the salivary glands *of* $Su(z)12^{3}/Su(z)12^{5}$ mutants (Fig. 4D), where 4E-BP is normally expressed. This result is consistent with the increase observed in S2 cells and suggests that PcG proteins not only silence *Thor* expression in imaginal discs, but modulate its expression level in tissues where it is expressed. The increase in 4E-BP protein level was confirmed by western (Fig. 4E).

Eliminating *Thor* in *E(z)* mutants partially rescues their small imaginal disc phenotype

The wing discs are among the largest discs in the developing larvae. The average surface area of the disc proper, not including the peripodial membrane, is just over 138,000 μm^2. Wing discs are also the most affected by E(Z) depletion, decreasing in area by 19 fold to an average area of just over 7,000 μm^2. Haltere and third leg discs are not as affected by E(Z) depletion but still decrease in area by 3.25 and 2.68 fold, respectively. Miron and colleagues (2001) previously showed that strong over-expressing of a modified form of *Drosophila* 4E-BP that binds more tightly to eIF4E in the wing disc dramatically decreased the overall size of the wing disc. We also found a significant decrease in wing disc size when over-expressing wild-type *4E-BP* with the strong *tub-GAL4* driver, but not the weaker *P{GawB}30A* imaginal disc GAL4 driver (Supplementary Fig. 5). Since *4E-BP* is ectopically expressed in the PRC2 mutant imaginal discs, it is possible that this causes the reduced growth of these discs. To test this, we eliminated the 4E-BP protein genetically in *E(z)* mutants by crossing *Thor (Thor^2* and *Thor^{1034})* mutations into the *E(z)^{63}*, *E(z)^5*, and *E(z)^{731}* mutant backgrounds. The area of the wing, haltere, and third leg discs of *Thor; E(z)* double mutants were compared to *E(z)* and *Thor* single homozygous mutants and wild-type (Oregon R) controls. The discs of *Thor; E(z)* double mutants displayed partial rescue of the small imaginal disc phenotype (Fig. 5), their mean area increasing 3.9 fold compared to the *E(z)* mutant, to an average area of 28,207 μm^2 (Figs 5A, B). The haltere and third leg discs of the *Thor; E(z)* double mutants increased by 1.73 and 1.83 fold, respectively (Fig 5C, D). The increase in area of these discs suggests that the derepression *of Thor* in the *E(z)* mutants is at least partly responsible for their small imaginal disc phenotype.

Since the decrease in *E(z)* mutant wing disc size is the result of a decrease in cell size (Fig. 1), we measured cell size in the partially rescued *Thor; E(z)* double mutants to determine if it was increased. Figure 5E shows that the size of mutant wing disc cells in the *Thor; E(z)* double mutant is significantly increased compared to *E(z)* single mutants, but is not as large as in wild-type, suggesting that additional factors also contribute to the small imaginal disc phenotype.

Eliminating *Thor* increases the frequency of pupariation in *E(z)* mutants

The small imaginal discs of *E(z)* mutants are not competent to differentiate into adult structures, even when cultured *in vivo* in wild type larval hosts (Shearn et al., 1978). As a consequence, *E(z)* mutants die in late third instar or after undergoing pupariation. 61.5% of *E(z)^5/E(z)^{63}* and *Df(3L)lxd6/E(z)^{63}* mutants (n ≥100 for each genotype) pupariate (Fig. 6), similar to results reported by Shearn and colleagues (1978). The majority of these never climb up the wall of their container and simply pupariate in the media. Some form an irregularly shaped curved puparium (similar to those described in Dolezal et al., 2005).

Eliminating *4E-BP* increased the fraction *of E(z)* mutants that pupariate to levels similar to wild-type (although many still pupariate in the media) (Fig. 6). However, it did not rescue their failure to pupate. This further suggests that while derepression of *Thor* in PRC2 mutants plays a role in their failure to pupariate, other functions required for initiating pupation and metamorphosis are perturbed in *E(z)* mutants.

Discussion

Polycomb Silencing of *Thor* regulates imaginal disc growth

This is the first report that Polycomb silencing regulates cell growth in *Drosophila*. The results presented here show that homozygous PRC2 subunit mutants have small imaginal discs due in part to a cell growth defect. Wing disc cells in *E(z)* mutants are only 25% of wild type wing cell size. This small disc phenotype is due in part to derepression of the *Thor* gene in imaginal discs, where it is normally transcriptionally silenced. We showed that the *Thor* gene is a direct target of Polycomb silencing in discs and that its expression is also modulated, but not silenced, by PcG proteins in S2 cells and possibly also in endoreduplicating larval cells. The *Thor* promoter region contains predicted binding sites for PHO, GAGA factor and several other factors associated with well-characterized PREs and is bound by PcG proteins in both S2 cells and imaginal discs. In Supplementary Fig. 4, PHOL ChIP-chip data from embryos (taken from Schuettengruber et al., 2009) show significant binding of PHOL to the *Thor* promoter. More recent ChIP-seq data (Enderle et al., 2011) (Supplementary Fig. 3), show that PC, PH, and TRX are also bound to the *Thor* promoter.

Eliminating 4E-BP in *E(z)* mutants partially rescues their small disc phenotype and increases the fraction of *E(z)* mutant larvae that pupariate. Previous studies have shown that wild type third instar imaginal discs whose size is reduced by radiation-induced apoptosis delay pupariation until the discs undergo compensatory proliferation to reach a critical size (Simpson et al., 1980; Stieper et al., 2008). Since complete absence of imaginal discs does not inhibit pupariation (Stieper et al., 2008), this suggests that the onset of pupariation is normally regulated by a signal released from the imaginal discs that inhibits pupariation until imaginal discs have reached a critical size. This might play a role in the increased frequency of pupariation in double mutants. However, *Thor; E(z)* double mutants still fail initiate metamorphosis, suggesting that despite their substantially larger size, these imaginal discs are still not competent to differentiate into adult structures. Given the large number of other genes that are directly or indirectly regulated by PcG proteins, this is perhaps not surprising. A similar phenomenon has been reported in $Bmi1^{-/-}$ and $Rnf2\ (Ring1b)^{-/-}$ mice (PSC and RING homologs). Null mutations in either *Bmi1* (Bruggeman et al., 2005) or *Rnf2* (Voncken et al., 2003) cause a cell proliferation defect that is only partially rescued by deletion of the *Ink4a/Arf* locus, a direct PcG target that encodes a potent cyclin dependent kinase inhibitor. The early developmental arrest of $Rnf2^{-/-}$ mice is only rescued to the E11/E12 stage after elimination of the *Ink4a/Arf* locus (Voncken et al., 2003).

Polycomb regulation of cell proliferation and growth

The leg, haltere and wing discs of *Thor; E(z)* double mutants are smaller than their wild type counterparts, despite their substantially increased size compared to *E(z)* single mutants, suggesting that they have other cell growth or cell proliferation defects. A number of genes that encode key regulators of cell proliferation, including *CycB*, *CycA*, *Myc*, and *upd*, have been shown to be directly regulated by PcG proteins (Oktaba et al., 2008; Classen et al., 2009; Goodliffe et al., 2005; Martinez et al., 2006). Genes encoding other regulators of cell proliferation, including *Rbf*, *E2F* and *Dp*, are bound by PcG proteins (Oktaba et al., 2008), suggesting that they may also be regulated by PcG proteins. However, derepression or

increased expression of most of these genes in PcG mutants would be unlikely to play a role in the small imaginal phenotype, since all but *Rbf promote* rather than inhibit cell proliferation. Moreover, none have been reported to show obvious difference in expression in *PcG* mutant clones in imaginal discs (Classen et al., 2009; Oktaba et. al., 2008). *Rbf* a key negative regulator of the cell cycle, does not alter imaginal disc size when intentionally over-expressed (Neufeld et al., 1998). Although this does not rule out a role for *Rbf in* the PRC2 small imaginal disc phenotype, there are likely to be other undiscovered genes that are directly or indirectly regulated by PcGs that play a role.

Absence of homeotic proteins in *E(z)* mutant discs

The small disc phenotype of PRC2 mutants is often attributed to derepression of more "posterior" homeotic genes typically seen in PcG mutant embryos and clones of mutant cells in third instar imaginal discs (Beuchle et al., 2001; Campbell et al., 1995; Gaytan de Ayala Alonso et al., 2007; Jurgens et al., 1984; McKeon and Brock, 1991; Simon et al., 1992). Homeotic transformation of the large wing disc to the smaller haltere disc in PcG mutants is due to derepression of *Ubx* in the wing disc (Birve et al., 2001; Gaytan de Ayala Alonso et al., 2007; Kurzhals et al., 2008; Pavlopoulos and Akam, 2011; Roch and Akam, 2000). However, *E(z)* mutant wing discs are four and a half times smaller than wild-type haltere discs of the same stage (Fig. 5) and are unable to differentiate into adult structures (Shearn et al., 1978). This would not be expected if they were simply transformed to haltere segmental identity. Surprisingly, Shearn and colleagues (1996) observed that the small imaginal discs *of E(z)* mutants contain no detectable SCR, ANTP, UBX, ABD-B or EN protein. The derepression of *Thor* in imaginal discs raises the possibility that the absence of detectable homeotic proteins could be due to 4E-BP-dependent inhibition of translation of their mRNAs. Interestingly, a *Ubx-lacZ* reporter containing the entire 35 kb of *Ubx* 5' regulatory sequence (including the *bxd* PRE) is expressed in these same *E(z)* mutant discs, suggesting that the endogenous *Ubx* mRNA is also likely to be present despite the absence of UBX protein (LaJeunesse and Shearn, 1996). The 5' UTRs of *Antp* and *Ubx* have been reported to contain internal ribosome entry sites (IRES) that might allow them to undergo cap-independent translation in certain tissues (Oh et al., 1992; Ye et al., 1997). However, Cavener and colleagues (1997) reported that while both of these IRESs promote capindependent translation in many larval tissues when present in a bicistronic reporter transgene, neither do so in imaginal discs under normal conditions.

The absence of homeotic proteins in imaginal discs of homozygous *E(z)* mutants stands in contrast to their presence in imaginal disc clones of homozygous PcG mutations, including *E(z)* and *Su(z)12* (Beuchle et al., 2001; Birve et al, 2001; Müller et al., 2002). In clones, the time required to detect derepression varies among homeotic genes and other Polycomb target genes (Beuchle et al., 2001), suggesting that it likely depends not only on the half life of residual wild type PcG protein in clones, but also on the different times required for full derepression of individual Polycomb target genes, as well as the rate of accumulation of their gene products once their derepression has occurred. Moreover, any translational inhibiting effect of derepressed *Thor* depends additionally on the accumulation of a sufficient amount of 4E-BP that has not been inactivated by phosphorylation by TOR kinase, which may introduce an additional time delay, depending on the status of TOR

pathway signaling. Interestingly, Beuchle et al. (2001), previously observed that derepression of *Ubx* was detectable in strong PcG mutant clones in the wing disc within 24 hours of clone induction; UBX protein level peaked by 72 hr, but then subsequently declined. Pavlopoulos and Akam (2011) reported that ectopic expression of *Ubx* in the wing disc also induced expression of *4E-BP*. The decline of UBX protein may reflect the onset of inhibition of *Ubx* mRNA translation by accumulating 4E-BP.

Temperature shift (t-s) experiments with homozygous temperature-sensitive *E(z)* mutants revealed that shifting to the restrictive temperature after the third instar molt results in wild-type sized discs that exhibit ectopic expression of SCR, ANTP, UBX or EN (Jones and Gelbart, 1990; LaJeunesse and Shearn, 1996), while shifting them before third instar results in small imaginal discs that contain no detectable homeotic proteins (LaJeunesse and Shearn, 1996). While perhaps puzzling at the time it was reported, this might hint that the time spent at the restrictive temperature determines whether derepression of *Thor* has occurred for long enough to allow sufficient 4E-BP to accumulate to have an impact on cell growth and translation. Moreover, in contrast to clones in imaginal discs, in t-s experiments E(Z) is inactivated in all cells, including the endoreduplicating larval cells, which might indirectly affect 4E-BP levels and phosphorylation state in mutant imaginal discs.

Why is the *Thor/4E-BP* gene a target of Polycomb silencing in imaginal discs?

Imaginal discs have been shown to be much less sensitive than the endoreduplicating larval tissues to the growth-inhibiting effects of temporary nutrient insufficiency. While the larval tissues undergo rapid growth arrest, the imaginal tissues continue to grow and proliferate, albeit at a slower rate (Britton and Edgar, 1998; Colombani et al., 2003; Zhang et al., 2000). Britton and Edgar (1998) have suggested that this may reflect the prioritization of the growth and development of adult progenitors, effectively re-allocating energy stores from endoreduplicating larval tissues to imaginal tissues and thus favoring survival of the larva to a reproductive adult in times of low nutrients. 4E-BP is expressed at substantial levels in some endoreduplicating larval tissues (Rodriguez et al., 1996; Teleman et al., 2005), allowing for a fast growth arrest response to the onset of nutrient insufficiency via the insulin-FOXO and TOR signaling pathways, the key sensors of nutrient availability. Polycomb silencing of *Thor* transcription in imaginal discs would render them refractory to both transcriptional activation of *Thor* by activated FOXO and the subsequent 4E-BP-mediated arrest of translation and cell growth in response to starvation (Fig. 7). Consistent with this, translation is not globally decreased in wing discs from wild type larvae fed only sucrose (Mirth et al., 2009). Thus Polycomb silencing of 4E-BP may constitute part of the mechanism for prioritizing growth of adult progenitors over larval tissues.

Modulation of 4E-BP expression by PcG proteins in larval tissues

Our major finding is that *Thor* is regulated by Polycomb silencing in imaginal discs. However, the endoreduplicating larval tissues, which normally express *4E-BP* at some level (Chintapalli et al., 2007; Rodriguez et al., 1996; Teleman et al., 2005), also exhibit elevated *4E-BP* levels in *Su(z)12* mutants (Fig. 4D), similar to what we observed in S2 cells after RNAi knockdown of PRC2 subunits (Fig. 3E). This is not surprising since the larval tissues of PRC2 subunit mutants also exhibit cell growth defects, including reduced cell size and

nuclear volume, as well as reduced polytenization of larval salivary gland chromosomes (Carrington and Jones, 1996), evident as reduced DAPI staining (DNA content) (Fig. 4D), indicative of having undergone fewer rounds of endoreduplication. This suggests that while PcG proteins silence *4E-BP* expression in the actively dividing imaginal disc cells, in S2 cells (Fig. 3E) and non-dividing endoreduplicating larval cells (Fig. 4D) they function as a transcriptional "governor" of *Thor*, modulating rather than completely silencing its expression. There are several examples of direct targets of Polycomb silencing that are not completely silenced (Bloyer et al., 2003; Oktaba et al., 2008; Park et al., 2012). However, *Thor* is the first example of a gene that is differentially regulated by PcG proteins in different tissues, possibly reflecting modes of PcG action that differ in detail in these different tissues. Polycomb proteins are bound to many target genes even when they are active. While this has been interpreted to mean that transcription does not necessarily preclude PcG protein binding, especially to PREs, it may be that this binding to active genes reflects more subtle modulation of transcription levels by PcG proteins, a phenomenon that may be more widespread that previously appreciated. Further investigation of *Thor* regulation will be required to determine what differences underlie its apparently different mode of regulation by PcG proteins in larval cells.

Supplementary Material

Refer to Web version on PubMed Central for supplementary material.

Acknowledgements

We thank P. Lasko, A. Shearn, R. Jones, and the Bloomington *Drosophila* Stock Center for reagents and *Drosophila* strains. We thank Carl Stratton and Vince Stepanik for technical assistance and Brian Bai for use of a Leica M16 microscope. We thank Peter C. Scacheri for smoothing and unlogging ChIP-chip data. This work was supported by NIH grant GM39255 to P.J.H.. H.M.S. was also supported by T32HD07104. Confocal and DM6000 microscopes used in this work were purchased with NIH shared instrumentation grants RR-021228-01 and RR-017980-01.

References

Bello B, Holbro N, Reichert H. Polycomb group genes are required for neural stem cell survival in postembryonic neurogenesis *of Drosophila* . Development. 2007; 134:1091–1099. [PubMed: 17287254]

Bernal A, Kimbrell DA. *Drosophila Thor* participates in host immune defense and connects a translational regulator with innate immunity. Proc. Natl. Acad. Sci. USA. 2000; 97:6019–6024. [PubMed: 10811906]

Bernal A, Schoenfeld R, Kleinhesselink K, Kimbrell DA. Loss *of Thor*, the single 4E-BP gene of *Drosophila*, does not result in lethality. D. I. S. 2004; 87:81–84.

Beuchle D, Struhl G, Muller J. Polycomb group proteins and heritable silencing of *Drosophila Hox* genes. Development. 2001; 128:993–1004. [PubMed: 11222153]

Birve A, Sengupta AK, Beuchle D, Larsson J, Kennison JA, Rasmuson-Lestander A, Muller J. *Su(z)12*, a novel *Drosophila* Polycomb group gene that is conserved in vertebrates and plants. Development. 2001; 128:3371–3379. [PubMed: 11546753]

Bloyer S, Cavalli G, Brock HW, Dura JM. Identification and characterization of' *polyhomeotic* PREs and TREs. Dev. Biol. 2003; 261:426–442. [PubMed: 14499651]

Boyer LA, Plath K, Zeitlinger J, Brambrink T, Medeiros LA, Lee TI, Levine SS, Wernig M, Tajonar A, Ray MK, Bell GW, Otte AP, Vidal M, Gifford DK, Young RA, Jaenisch R. Polycomb

complexes repress developmental regulators in murine embryonic stem cells. Nature. 2006; 441:349–353. [PubMed: 16625203]

Bracken AP, Dietrich N, Pasini D, Hansen KH, Helin K. Genome-wide mapping of Polycomb target genes unravels their roles in cell fate transitions. Genes Dev. 2006; 20:1123–1136. [PubMed: 16618801]

Britton JS, Edgar BA. Environmental control of the cell cycle in *Drosophila:* nutrition activates mitotic and endoreplicative cells by distinct mechanisms. Development. 1998; 125:2149–2158. [PubMed: 9570778]

Brown JL, Fritsch C, Mueller J, Kassis JA. The *Drosophila pho-like* gene encodes a YY1-related DNA binding protein that is redundant with pleiohomeotic in homeotic gene silencing. Development. 2003; 130:285–294. [PubMed: 12466196]

Brown JL, Mucci D, Whiteley M, Dirksen ML, Kassis JA. The *Drosophila* Polycomb group gene *pleiohomeotic* encodes a DNA binding protein with homology to the transcription factor YY1. Mol. Cell. 1998; 1:1057–64. [PubMed: 9651589]

Brown JL, Kassis JA. Spps, a Drosophila Sp1/KLF family member, binds to PREs and is required for PRE activity late in development. Development. 2010; 137:2597–2602. [PubMed: 20627963]

Bruggeman SW, Valk-Lingbeek ME, van der Stoop PP, Jacobs JJ, Kieboom K, Tanger E, Hulsman D, Leung C, Arsenijevic Y, Marino S, van Lohuizen M. Ink4a and Arf differentially affect cell proliferation and neural stem cell self-renewal in Bmi1-deficient mice. Genes Dev. 2005; 12:1438–1443. [PubMed: 15964995]

Busturia A, Lloyd A, Bejarano F, Zavortink M, Xin H, Sakonju S. The MCP silencer of the *Drosophila Abd-B* gene requires both Pleiohomeotic and GAGA factor for the maintenance of repression. Development. 2001; 128:2163–2173. [PubMed: 11493537]

Campbell RB, Sinclair DAR, Couling M, Brock HW. Genetic interactions and dosage effects of Polycomb group genes *of Drosophila* . Mol. and Gen. Genetics. 1995; 246:291–300.

Cao R, Wang L, Wang H, Xia L, Erdjument-Bromage H, Tempst P, Jones RS, Zhang Y. Role of histone H3 lysine 27 methylation in Polycomb-group silencing. Science. 2002; 298:1039–1043. [PubMed: 12351676]

Carrington EA, Jones RS. The *Drosophila Enhancer of zeste* gene encodes a chromosomal protein: examination of wild-type and mutant protein distribution. Development. 1996; 122:4073–4083. [PubMed: 9012527]

Chan CS, Rastelli L, Pirrotta V. A Polycomb response element in the *Ubx* gene that determines an epigenetically inherited state of repression. EMBO J. 1994; 13:2553–2564. [PubMed: 7912192]

Chanas G, Maschat F. Tissue specificity of hedgehog repression by the Polycomb group during *Drosophila melanogaster* development. Mech. Dev. 2005; 122:975–987. [PubMed: 16024236]

Chintapalli VR, Wang J, Dow JA. Using Fly Atlas to identify better *Drosophila melanogaster* models of human disease. Nat. Genet. 2007; 39:715–720. [PubMed: 17534367]

Christen B, Bienz M. Imaginal disc silencers from Ultrabithorax: evidence for Polycomb response elements. Mech. Dev. 1994; 48:255–266. [PubMed: 7893606]

Classen AK, Bunker BD, Harvey KF, Vaccari T, Bilder D. A tumor suppressor activity of *Drosophila Polycomb* genes mediated by JAK-STAT signaling. Nat. Genet. 2009; 41:1150–1155. [PubMed: 19749759]

Colombani J, Raisin S, Pantalacci S, Radimerski T, Montagne J, Leopold P. A nutrient sensor mechanism controls *Drosophila* growth. Cell. 2003; 114:739–749. [PubMed: 14505573]

Cunningham MDJ, Lesley Brown JL, Judith A, Kassis JA. Characterization of the Polycomb group response elements of the *Drosophila melanogaster invected locus* . Mol. Cell. Biol. 2010; 30:820–828. [PubMed: 19948883]

Czermin B, Melfi R, McCabe D, Seitz V, Imhof A, Pirrotta V. *Drosophila* enhancer of Zeste/ESC complexes have a histone H3 methyltransferase activity that marks chromosomal Polycomb sites. Cell. 2002; 111:185–196. [PubMed: 12408863]

Dejardin J, Rappailles A, Cuvier O, Grimaud C, Decoville M, Locker D, Cavalli G. Recruitment of *Drosophila* Polycomb group proteins to chromatin by DSP1. Nature. 2005; 434:533–538. [PubMed: 15791260]

Dellino GI, Tatout C, Pirrotta V. Extensive conservation of sequences and chromatin structures in the *bxd* Polycomb Response Element among *Drosophilid* species. Int. J. Dev. Biol. 2002; 46:133–141. [PubMed: 11902674]

DeSanta F, Totaro MG, Prosperini E, Notarbartolo S, Testa G, Natoli G. The histone H3 lysine-27 demethylase Jmjd3 links inflammation to inhibition of Poly comb-mediated gene silencing. Cell. 2007; 130:1083–1094. [PubMed: 17825402]

Dolezal T, Dolezelova E, Zurovec M, Bryant PJ. A role for adenosine deaminase in *Drosophila* larval development. PLoS Biol. 2005; 3:e201. [PubMed: 15907156]

Enderle D, Beisel C, Stadler MB, Gerstung M, Athri P, Paro R. Polycomb preferentially targets stalled promoters of coding and noncoding transcripts. Genome Res. 2011; 21:216–226. [PubMed: 21177970]

Fang J, Chen T, Chadwick B, Li E, Zhang Y. Ring1b-mediated H2A ubiquitination associates with inactive X chromosomes and is involved in initiation of X inactivation. J. Biol. Chem. 2004; 279:52812–52815. [PubMed: 15509584]

Fiedler T, Rehmsmeier M. jPREdictor: a versatile tool for the prediction of *cis*-regulatory elements. Nucleic Acids Res. 2006; 34:546–550.

Gatti M, Baker BS. Genes controlling essential cell-cycle functions in *Drosophila melanogaster* . Genes Dev. 1989; 3:438–453. [PubMed: 2498166]

Gaytan de Ayala Alonso A, Gutierrez L, Fritsch C, Papp B, Beuchle D, Muller J. A genetic screen identifies novel Polycomb group genes in *Drosophila* . Genetics. 2007; 176:2099–2108. [PubMed: 17717194]

Goodliffe JM, Wieschaus E, Cole MD. Polycomb mediates *Myc* autorepression and its transcriptional control of many loci *in Drosophila* . Genes Dev. 2005; 19:2941–2946. [PubMed: 16357214]

Gutiérrez L, Oktaba K, Scheuermann JC, Gambetta MC, Ly-Hartig N, Müller J. The role of the histone H2A ubiquitinase Sce in Polycomb repression. Development. 2012; 139:117–127. [PubMed: 22096074]

Gutjahr T, Frei E, Spicer C, Baumgartner S, White RA, Noll M. The Polycomb-group gene, *extra sex combs*, encodes a nuclear member of the WD-40 repeat family. EMBO J. 1995; 14:4296–4306. [PubMed: 7556071]

Herz HM, Mohan M, Garrett AS, Miller C, Casto D, Zhang Y, Seidel C, Haug JS, Florens L, Washburn MP, Yamaguchi M, Shiekhattar R, Shilatifard A. Polycomb repressive complex 2-dependent and -independent functions of Jarid2 in transcriptional regulation in *Drosophila* . Mol. Cell Biol. 2012; 32:1683–1693. [PubMed: 22354997]

Hagstrom K, Muller M, Schedl P. A Polycomb and GAGA dependent silencer adjoins the *Fab-7* boundary in the *Drosophila* bithorax complex. Genetics. 1997; 146:1365–1380. [PubMed: 9258680]

Hauenschild A, Ringrose L, Altmutter C, Paro R, Rehmsmeier M. Evolutionary plasticity of Polycomb/Trithorax response elements in *Drosophila* species. PLoS Biol. 2008; 6:e261. [PubMed: 18959483]

Hodgson JW, Argiropoulos B, Brock HW. Site-specific recognition of a 70-base-pair element containing d(GA)(n) repeats mediates bithoraxoid polycomb group response element-dependent silencing. Mol. Cell. Biol. 2001; 21:4528–4543. [PubMed: 11416132]

Holmes AM, Weedmark KA, Gloor GB. Mutations in the *extra sex combs* and *Enhancer of Polycomb* genes increase homologous recombination in somatic cells *of Drosophila melanogaster* . Genetics. 2006; 172:2367–2377. [PubMed: 16452150]

Horard B, Tatout C, Poux S, Pirrotta V. Structure of a Polycomb response element and in vitro binding of Polycomb group complexes containing GAGA factor. Mol. Cell. Biol. 2000; 20:3187–3197. [PubMed: 10757803]

Jones RS, Gelbart WM. Genetic analysis of the *enhancer of zeste* locus and its role in gene regulation in *Drosophila melanogaster* . Genetics. 1990; 126:185–199. [PubMed: 1977656]

Jurgens G, Wieschaus E, Nusslein-Volhard C, Kluding H. Mutations affecting the pattern of the larval cuticle in *Drosophila melanogaster* . Roux's Archives of Dev. Biol. 1984; 193:283–295.

Ketel CS, Andersen EF, Vargas ML, Suh J, Strome S, Simon JA. Subunit contributions to histone methyltransferase activities of fly and worm Polycomb group complexes. Mol. Cell. Biol. 2005; 25:6857–6868. [PubMed: 16055700]

Klymenko T, Papp B, Fischle W, Kocher T, Schelder M, Fritsch C, Wild B, Wilm M, Muller J. A Polycomb group protein complex with sequence-specific DNA-binding and selective methyl-lysine-binding activities. Genes Dev. 2006; 20:1110–1122. [PubMed: 16618800]

Kurzhals RL, Tie F, Stratton CA, Harte PJ. *Drosophila* ESC-like can substitute for ESC and becomes required for Polycomb silencing if ESC is absent. Dev. Biol. 2008; 313:293–306. [PubMed: 18048023]

LaJeunesse D, Shearn A. *E(z):* a Polycomb group gene or a Trithorax group gene? Development. 1996; 122:2189–2197. [PubMed: 8681799]

Lehmann L, Ferrari R, Vashisht AA, Wohlschlegel JA, Kurdistani SK, Carey M. Polycomb Repressive Complex 1 (PRC1) Disassembles RNA Polymerase II Preinitiation Complexes. J. Biol. Chem. 2012; 287:35784–35794. [PubMed: 22910904]

Lee TI, Jenner RG, Boyer LA, Guenther MG, Levine SS, Kumar RM, Chevalier B, Johnstone SE, Cole MF, Isono K, Koseki H, Fuchikami T, Abe K, Murray HL, Zucker JP, Yuan B, Bell GW, Herbolsheimer E, Hannett NM, Sun K, Odom DT, Otte AP, Volkert TL, Bartel DP, Melton DA, Gifford DK, Jaenisch R, Young RA. Control of developmental regulators by Polycomb in human embryonic stem cells. Cell. 2006; 125:301–313. [PubMed: 16630818]

Mahmoudi T, Zuijderduijn LM, Mohd-Sarip A, Verrijzer CP. GAGA facilitates binding of Pleiohomeotic to a chromatinized Polycomb response element. Nucleic Acids Res. 2003; 31:4147–4156. [PubMed: 12853632]

Mak W, Baxter J, Silva J, Newall AE, Otte AP, Brockdorff N. Mitotically stable association of Polycomb group proteins EED and Enx1 with the inactive X chromosome in trophoblast stem cells. Curr. Biol. 2002; 12:1016–1020. [PubMed: 12123576]

Martinez AM, Colomb S, Dejardin J, Bantignies F, Cavalli G. Polycomb group-dependent Cyclin A repression in *Drosophila* . Genes Dev. 2006; 20:501–513. [PubMed: 16481477]

Maurange C, Lee N, Paro R. Signaling meets chromatin during tissue regeneration in *Drosophila* . Curr. Opin. Genet. Dev. 2006; 16:485–489. [PubMed: 16919444]

McKeon J, Brock HW. Interactions of the Polycomb group of genes with homeotic loci of *Drosophila* . Roux's Arch. Dev. Biol. 1991; 199:387–396.

Miron M, Lasko P, Sonenberg N. Signaling from Akt to FRAP/TOR targets both 4E-BP and S6K in *Drosophila melanogaster* . Mol. Cell. Biol. 2003; 23:9117–9126. [PubMed: 14645523]

Miron M, Verdu J, Lachance PE, Birnbaum MJ, Lasko PF, Sonenberg N. The translational inhibitor 4E-BP is an effector of PI(3)K/Akt signaling and cell growth in *Drosophila* . Nat. Cell. Biol. 2001; 3:596–601. [PubMed: 11389445]

Mirth CK, Truman JW, Riddiford LM. The ecdysone receptor controls the post-critical weight switch to nutrition-independent differentiation in *Drosophila* wing imaginal discs. Development. 2009; 136:2345–2353. [PubMed: 19515698]

Mohd-Sarip A, Cleard F, Mishra RK, Karch F, Verrijzer CP. Synergistic recognition of an epigenetic DNA element by Pleiohomeotic and a Polycomb core complex. Genes Dev. 2005; 19:1755–1760. [PubMed: 16077005]

Mohd-Sarip A, van der Knaap JA, Wyman C, Kanaar R, Schedl P, Verrijzer CP. Architecture of a Polycomb nucleoprotein complex. Mol. Cell. 2006; 24:91–100. [PubMed: 17018295]

Müller J, Hart CM, Francis NJ, Vargas ML, Sengupta A, Wild B, Miller EL, O'Connor MB, Kingston RE, Simon JA. Histone methyltransferase activity *of a Drosophila* Polycomb group repressor complex. Cell. 2002; 111:197–208. [PubMed: 12408864]

Nekrasov M, Wild B, Müller J. Nucleosome binding and histone methyltransferase activity of *Drosophila* PRC2. EMBO Rep. 2005; 6:348–353. [PubMed: 15776017]

Neufeld TP, de la Cruz AF, Johnston LA, Edgar BA. Coordination of growth and cell division in the *Drosophila* wing. Cell. 1998; 93:1183–1193. [PubMed: 9657151]

Oh SK, Scott MP, Sarnow P. Homeotic gene *Antennapedia* mRNA contains 5'-noncoding sequences that confer translational initiation by internal ribosome binding. Genes Dev. 1992; 6:1643–1653. [PubMed: 1355457]

Ohno K, McCabe D, Czermin B, Imhof A, Pirrotta V. ESC, ESCL and their roles in Polycomb Group mechanisms. Mech. Dev. 2008; 125:527–541. [PubMed: 18276122]

Oktaba K, Gutierrez L, Gagneur J, Girardot C, Sengupta AK, Furlong EE, Müller J. Dynamic regulation by Polycomb group protein complexes controls pattern formation and the cell cycle in *Drosophila* . Dev. Cell. 2008; 15:877–889. [PubMed: 18993116]

Park SY, Schwartz YB, Kahn TG, Asker D, Pirrotta V. Regulation of Polycomb group genes *Psc* and *Su(z)2* in Drosophila melanogaster. Mech. Dev. 2012; 128:536–547. [PubMed: 22289633]

Pasini D, Bracken AP, Hansen JB, Capillo M, Helin K. The Polycomb group protein Suz12 is required for embryonic stem cell differentiation. Mol. Cell. Biol. 2007; 27:3769–3779. [PubMed: 17339329]

Pavlopoulos A, Akam M. Hox gene *Ultrabithorax* regulates distinct sets of target genes at successive stages *of Drosophila* haltere morphogenesis. Proc. Natl. Acad. Sci. U.S.A. 2011; 108:2855–2860. [PubMed: 21282633]

Phillips MD, Shearn A. Mutations in *polycombeotic, a Drosophila* Polycomb-group gene, cause a wide range of maternal and zygotic phenotypes. Genetics. 1990; 125:91–101. [PubMed: 2341036]

Ringrose L, Rehmsmeier M, Dura JM, Paro R. Genome-wide prediction of Polycomb/Trithorax response elements in *Drosophila melanogaster* . Dev. Cell. 2003; 5:759–771. [PubMed: 14602076]

Roch F, Akam M. Ultrabithorax and the control of cell morphology in *Drosophila* halteres. Development. 2000; 127:97–107. [PubMed: 10654604]

Rodriguez A, Zhou Z, Tang ML, Meller S, Chen J, Bellen H, Kimbrell DA. Identification of immune system and response genes, and novel mutations causing melanotic tumor formation in *Drosophila melanogaster* . Genetics. 1996; 143:929–940. [PubMed: 8725239]

Schmitges FW, Prusty AB, Faty M, Stützer A, Lingaraju GM, Aiwazian J, Sack R, Hess D, Li L, Zhou S, Bunker RD, Wirth U, Bouwmeester T, Bauer A, Ly-Hartig N, Zhao K, Chan H, Gu J, Gut H, Fischle W, Müller J, Thomä NH. Histone methylation by PRC2 is inhibited by active chromatin marks. Mol. Cell. 2011; 42:330–341. [PubMed: 21549310]

Schuettengruber B, Ganapathi M, Leblanc B, Portoso M, Jaschek R, Tolhuis B, van Lohuizen M, Tanay A, Cavalli G. Functional anatomy of polycomb and trithorax chromatin landscapes in *Drosophila* embryos. PLoS Biol. 2009; 7:146–163.

Schwartz YB, Kahn TG, Nix DA, Li XY, Bourgon R, Biggin M, Pirrotta V. Genome-wide analysis of Polycomb targets in *Drosophila melanogaster* . Nat. Genet. 2006; 38:700–705. [PubMed: 16732288]

Schwartz YB, Pirrotta V. Polycomb silencing mechanisms and the management of genomic programmes. Nat. Rev. Genet. 2007; 8:9–22. [PubMed: 17173055]

Schwartz YB, Pirrotta V. Polycomb complexes and epigenetic states. Curr. Opin. Cell Biol. 2008; 20:266–273. [PubMed: 18439810]

Schwartz YB, Kahn TG, Stenberg P, Ohno K, Bourgon R, Pirrotta V. Alternative epigenetic chromatin states of polycomb target genes. PLoS Genet. 2010; 6:e1000805. [PubMed: 20062800]

Shaw T, Martin P. Epigenetic reprogramming during wound healing: loss of Polycomb-mediated silencing may enable upregulation of repair genes. EMBO Rep. 2009; 10:881–886. [PubMed: 19575012]

Shearn A, Hersperger G, Hersperger E, Pentz ES, Denker P. Multiple allele approach to the study of genes in *Drosophila melanogaster* that are Involved in imaginal disc development. Genetics. 1978; 89:355–370. [PubMed: 17248839]

Simon J, Chiang A, Bender W. Ten different Polycomb group genes are required for spatial control of the *abdA* and *AbdB* homeotic products. Development. 1992; 114:493–505. [PubMed: 1350533]

Simon J, Chiang A, Bender W, Shimell MJ, O'Connor M. Elements of the *Drosophila* bithorax complex that mediate repression by Polycomb group products. Dev. Biol. 1993; 158:131–144. [PubMed: 8101171]

Simon JA, Lange CA. Roles of the EZH2 histone methyltransferase in cancer epigenetics. Mutat. Res. 2008; 647:21–29. [PubMed: 18723033]

Simpson P, Berreur P, Berreur-Bonnenfant J. The initiation of pupariation *in Drosophila:* dependence on growth of the imaginal discs. J. Embryol. Exp. Morphol. 1980; 57:155–165. [PubMed: 7430927]

Sparmann A, van Lohuizen M. Polycomb silencers control cell fate, development and cancer. Nat. Rev. Cancer. 2006; 6:846–856. [PubMed: 17060944]

Stieper BC, Kupershtok M, Driscoll MV, Shingleton AW. Imaginal discs regulate developmental timing in *Drosophila melanogaster* . Dev. Biol. 2008; 321:18–26. [PubMed: 18632097]

Struhl G. Role of the *esc+* gene product in ensuring the selective expression of segment-specific homeotic genes in *Drosophila* . J. Embryol. Exp. Morphol. 1983; 76:297–331. [PubMed: 6631324]

Strutt H, Cavalli G, Paro R. Co-localization of Polycomb protein and GAGA factor on regulatory elements responsible for the maintenance of homeotic gene expression. EMBO J. 1997; 16:3621–3632. [PubMed: 9218803]

Teleman AA, Chen YW, Cohen SM. 4E-BP functions as a metabolic brake used under stress conditions but not during normal growth. Genes Dev. 2005; 19:1844–1848. [PubMed: 16103212]

Tettweiler G, Miron M, Jenkins M, Sonenberg N, Lasko PF. Starvation and oxidative stress resistance in *Drosophila* are mediated through the eIF4E-binding protein, d4E-BP. Genes Dev. 2005; 19:1840–1843. [PubMed: 16055649]

Tie F, Furuyama T, Harte PJ. The *Drosophila* Polycomb Group proteins ESC and E(Z) bind directly to each other and co-localize at multiple chromosomal sites. Development. 1998; 125:3483–3496. [PubMed: 9693151]

Tie F, Furuyama T, Prasad-Sinha J, Jane E, Harte PJ. The *Drosophila* Polycomb Group proteins ESC and E(Z) are present in a complex containing the histone-binding protein p55 and the histone deacetylase RPD3. Development. 2001; 128:275–286. [PubMed: 11124122]

Tie F, Siebold AP, Harte PJ. The N-terminus *of Drosophila* ESC mediates its phosphorylation and dimerization. Biochem. Biophys. Res. Commun. 2005; 332:622–632. [PubMed: 15896722]

Tie F, Stratton CA, Kurzhals RL, Harte PJ. The N terminus *of Drosophila* ESC binds directly to histone H3 and is required for E(Z)-dependent trimethylation of H3 lysine 27. Mol. Cell. Biol. 2007; 27:2014–2026. [PubMed: 17210640]

Tie F, Banerjee R, Stratton CA, Prasad-Sinha J, Stepanik V, Zlobin A, Diaz MO, Scacheri PC, Harte PJ. CBP-mediated acetylation of histone H3 lysine 27 antagonizes *Drosophila* Polycomb silencing. Development. 2009; 136:3131–3141. [PubMed: 19700617]

Voncken JW, Roelen BA, Roefs M, de Vries S, Verhoeven E, Marino S, Deschamps J, van Lohuizen M. Rnf2 (Ring1b) deficiency causes gastrulation arrest and cell cycle inhibition. Proc. Natl. Acad. Sci. USA. 2003; 5:2468–2473. [PubMed: 12589020]

Wang J, Mager J, Chen Y, Schneider E, Cross JC, Nagy A, Magnuson T. Imprinted X inactivation maintained by a mouse Polycomb group gene. Nat. Genet. 2001; 28:371–375. [PubMed: 11479595]

Wang L, Brown JL, Cao R, Zhang Y, Kassis JA, Jones RS. Hierarchical recruitment of Polycomb group silencing complexes. Mol. Cell. 2004; 14:637–646. [PubMed: 15175158]

Wang L, Jahren N, Vargas ML, Andersen EF, Benes J, Zhang J, Miller EL, Jones RS, Simon JA. Alternative ESC and ESC-like subunits of a Polycomb group histone methyltransferase complex are differentially deployed during *Drosophila* development. Mol. Cell Biol. 2006; 26:2637–2647. [PubMed: 16537908]

Ye X, Fong P, Iizuka N, Choate D, Cavener DR. *Ultrabithorax* and *Antennapedia* 5’ untranslated regions promote developmentally regulated internal translation initiation. Mol. Cell. Biol. 1997; 17:1714–1721. [PubMed: 9032298]

Zhang H, Stallock JP, Ng JC, Reinhard C, Neufeld TP. Regulation of cellular growth by the *Drosophila* target of rapamycin dTOR. Genes Dev. 2000; 14:2712–2724. [PubMed: 11069888]

Zhao J, Sun BK, Erwin JA, Song JJ, Lee JT. Polycomb proteins targeted by a short repeat RNA to the mouse X chromosome. Science. 2008; 322:750–756. [PubMed: 18974356]

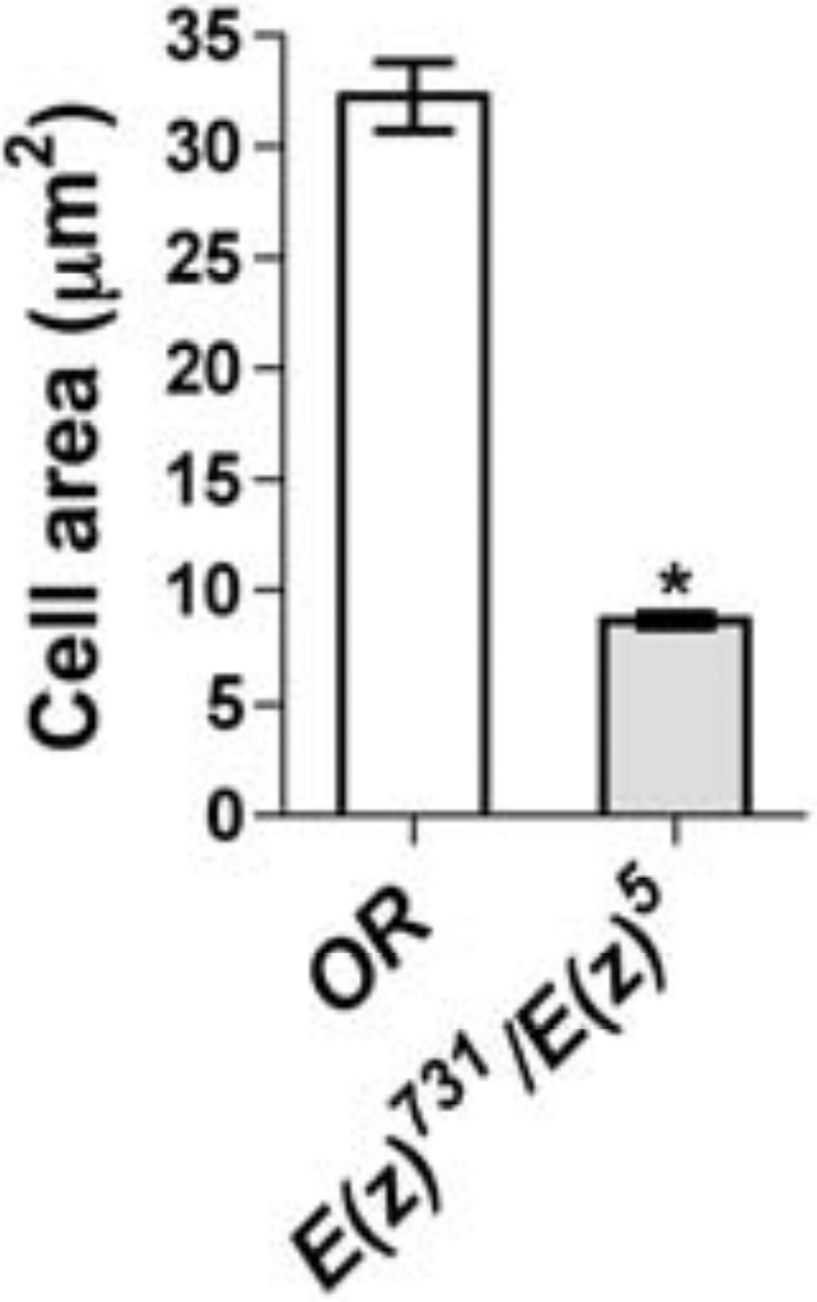

Fig. 1. The cell size is reduced in the wing disc cells of *E(z)* mutants

Wing discs of each genotype were stained with phalloidin to visualize the cell membrane. Error bars represent standard error of the mean. The area of wing disc cells is used as a proxy for cell volume. An asterisk represents a statistically significant difference (T-test) from the control Oregon-R ($P < 0.0001$).

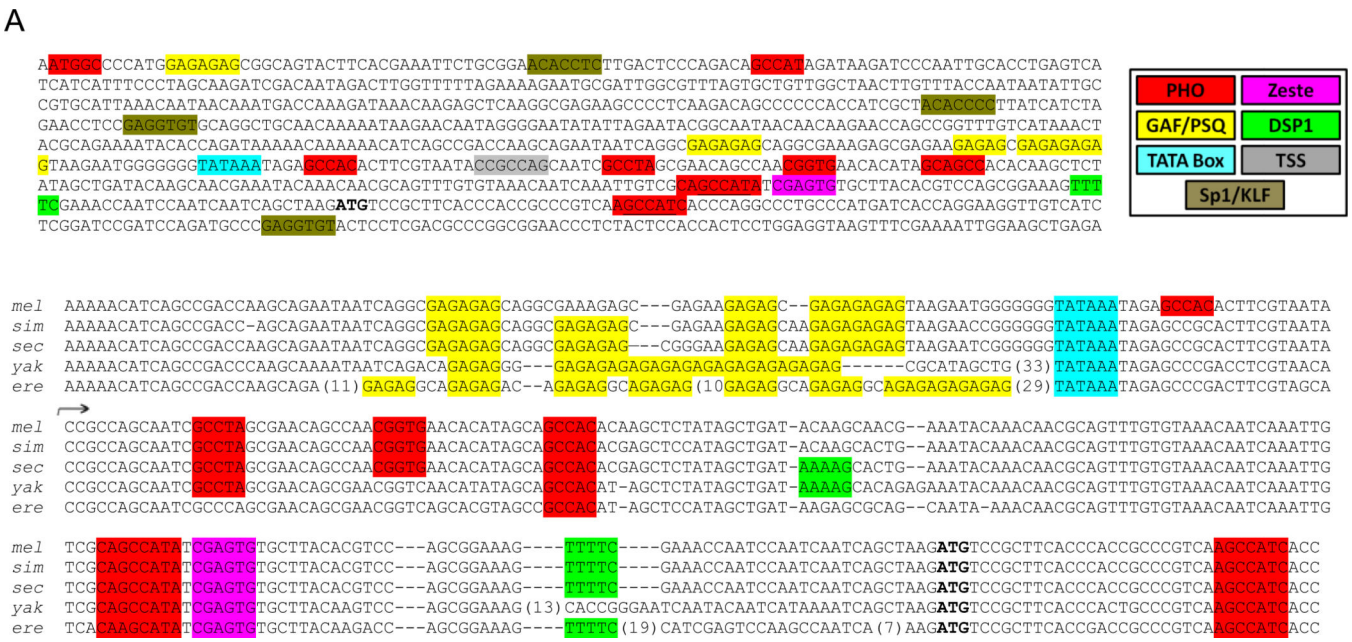

Fig. 2. Sequence alignment of the DNA binding protein motifs upstream of the *Thor* gene

(A) DNA binding sites for PHO/PHOL (Red), GAF or PSQ (Yellow), Sp1/KLF(Brown), Zeste (Purple) and DSP1 (Green) are shown to surround the TATA Box (Blue) and TSS (Grey). The genomic region shown includes nucleotide positions 3478403-3478683 (AE014134). The underlined text is the PHO core consensus sequence. The initiation codon is in bold text. (B) A multiple species comparison of the *Thor* promoter between four different, divergent *Drosophila* species shows the conserved DNA binding sites, indicated by color in legend (right). Numbers in parentheses indicate amount of nucleotides removed for alignment. The first codon is in bold text. An arrow depicts the TSS. Sp1/KLF motifs were not analyzed for this data set.

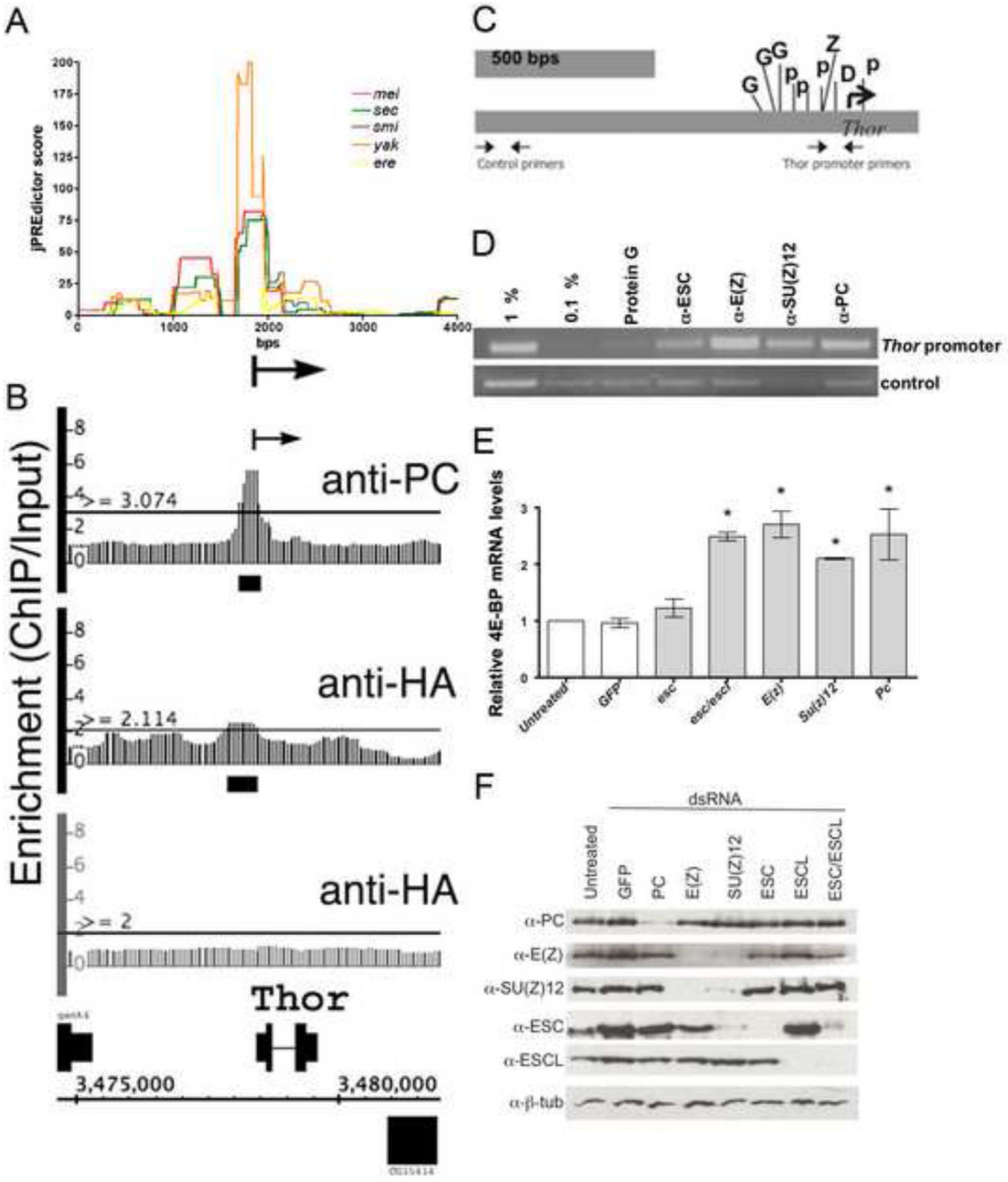

Fig. 3. PcG proteins bind the *Thor* promoter and modulate *4E-BP* mRNA level in S2 cells

(A) A graphical representation of the jPREdictor score across the *Thor* gene *for Drosophila melanogaster* and the four most closely related *Drosophila* species. The arrow depicts the *Thor* promoter. (B) ChIP-chip results for the *Thor* gene in S2 cells (top and bottom) and a stable S2 cell line expressing HA-PC from the *Act5C* promoter (middle). Anti-PC and anti-HA antibodies used in immunoprecipitation are indicated on the right of each plot. The bottom plot is a negative control using normal S2 cells and the anti-HA antibody. The horizontal line delimits the top 1% of signals genome-wide. Bar below each plot indicates

PC-enriched sites (≥ 99%). The *Thor* transcription unit is indicated by horizontal arrow (vertical line at its transcription start site) on top. All genes present in this region are indicated at bottom of figure. (C) A depiction of the *Thor* promoter. This shows the location of the *Thor* promoter and control primers used in the ChIP PCR and qPCR experiments. The location of GAF (G), PHO/PHOL (P), Zeste (Z), DSP1 (D) binding sites are shown. The arrow above the gene indicates the TSS. (D) Soluble chromatin was immunoprecipitated from S2 cells with protein G beads (Lane 3, negative control) or antibodies to PcG proteins; ESC (Lane 4), E(Z) (Lane 5), SU(Z)12 (Lane 6), or PC (Lane 7). Immunoprecipitates were subjected to PCR with a primer-pair specific to the *Thor* promoter (top row) or 1 kb upstream of *Thor* (negative control as shown on ChIP-chip, bottom row). PCR was also preformed on 1% of the total input (Lane 1, positive signal) and 0.1% of the total input (Lane 2, negative threshold). (E) Relative *4E-BP* mRNA levels, determined by real-time qRT-PCR, in S2 cells depleted of the PcG proteins listed on the x-axis by RNAi knockdown. The values were normalized to *RpS12* mRNA. Error bars indicate standard error of the mean. An asterisk indicates a statistically significant difference (T-test) from the control ($P < 0.05$). (F) Western blot showing degree of depletion of PcG proteins in dsRNA treated S2 cells.

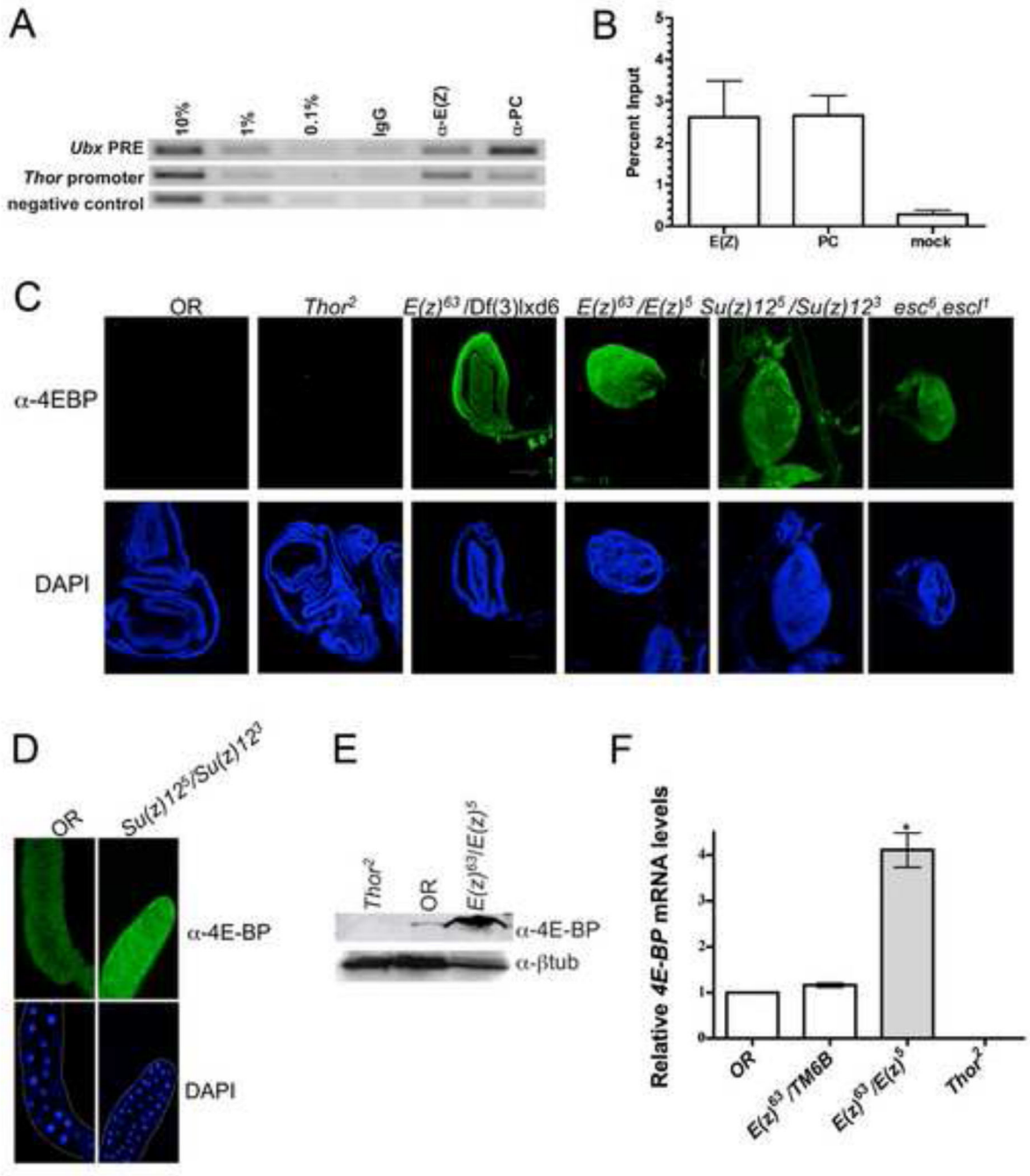

Fig. 4. PcG proteins bind the *Thor* promoter and silence *4E-BP* expression in imaginal discs

(A,B) Soluble chromatin was immunoprecipitated from the imaginal discs (along with some attached CNS tissue) of wandering third-instar larva using antibodies to PcG proteins; E(Z) (Lane 5) or PC (Lane 6) or E(Z) preimmune serum ("IgG", Lane 4, negative control also referred to as mock). (A) PCR analysis (shown inverted) was performed on immunoprecipitated chromatin with primers for the *Ubx* PRE (first row, positive control), *Thor* promoter (second row) (primers shown in Fig. 3C), or a region on Chromosome 3L shown to not bind PcG proteins by ChIP-chip (Feng Tie, unpublished) (third row, negative

control). PCR was also preformed on 10% of the total input (Lane 1, positive signal), 1% of the total input (Lane 2, positive signal), and 0.1% of the total input (Lane 2, negative threshold). (B) Real time q-PCR analysis using *Thor* promoter primers (primers shown in Fig. 3C) was performed showing increased binding of E(Z) and PC protein compared to a mock pull-down using IgG to the *Thor* promoter. (C) Imaginal discs from wandering, third-instar larvae were dissected and stained with 4E-BP antiserum (Green, top row) or DAPI (Blue, bottom row) to mark nuclei. All images were taken on a confocal microscope at 40X. (D) Salivary glands from wandering, third-instar larvae were dissected and stained with 4E-BP antiserum (Green, top row) or DAPI (Blue, bottom row) to mark nuclei. All images were taken on a confocal microscope at 20X. (E) Western analysis of 4E-BP protein levels (top row) from whole wandering, third-instar larval extracts of $Thor^{2}$ (Lane 1, negative control), OR (Lane 2), and $E(z)^{63}/E(z)^{5}$ (Lane 3). β-Tubulin was used as a loading control (bottom row). (F) Real Time qRT-PCR analysis *of 4E-BP* mRNA levels in the imaginal disc and brain tissues from wandering, third-instar larva of $Thor^{2}$ (Lane 4, negative control), $E(z)^{63}$/*TM6B* (Lane 2), and $E(z)^{63}/E(z)^{5}$ (Lane 3) was compared to that of Oregon-R (OR) (Lane 1). The values were normalized to *Rsp12* mRNA. Error bars represent standard error of the mean. An asterisk represents a statistically significant difference (T-test) from the control Oregon-R ($P < 0.0006$).

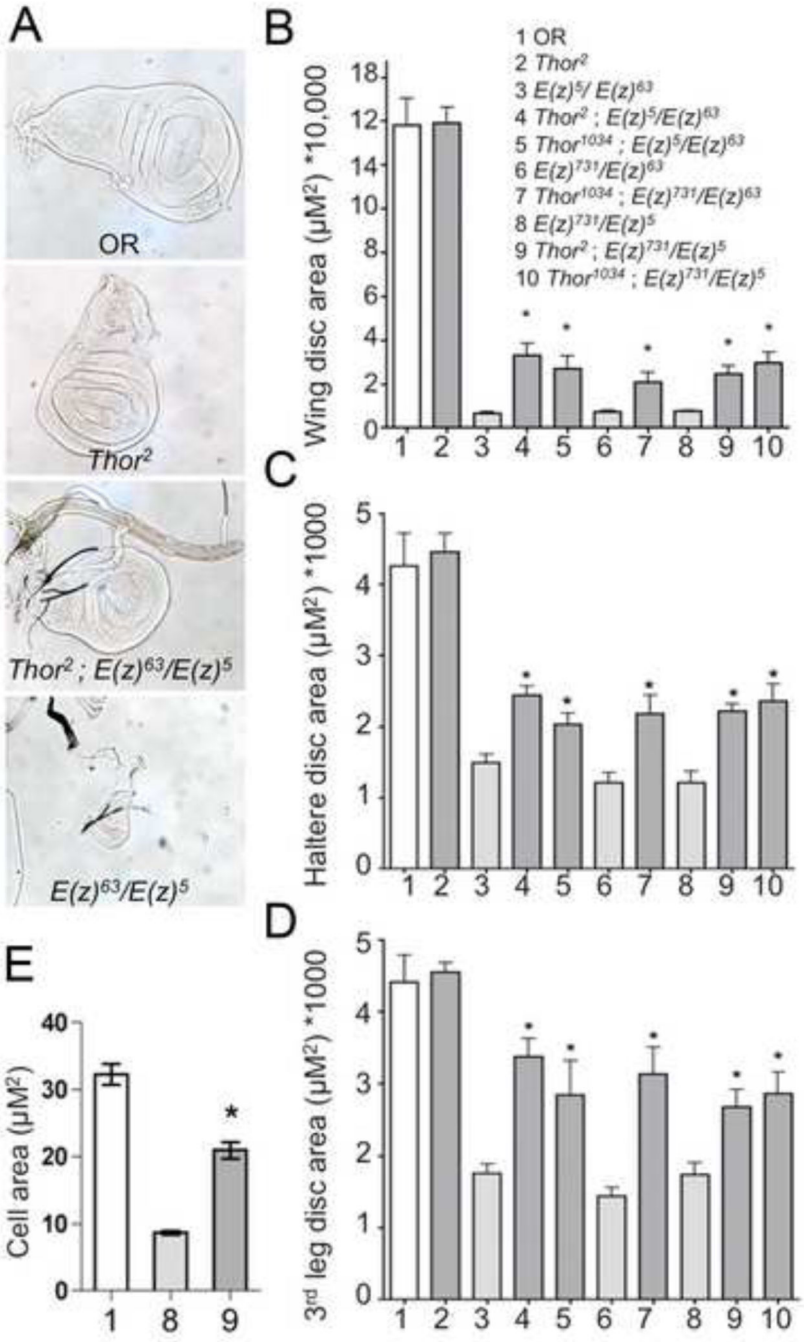

Fig. 5. Elimination of *Thor* in *E(z)* mutants partially rescues the reduced imaginal disc area

(A) The photos show the wing discs of wandering, third instar larva of the following genotypes; OR, $Thor^2$, $Thor^2$; $E(z)^{63}/E(z)^5$ and $E(z)^{63}/E(z)^5$. All images were taken at 10X using brightfield microscopy. (B, C, D) The area of the wing discs (B) haltere discs (C), or 3^r leg discs (D) in μm^2 of OR (Lane 1), $Thor^2$ (Lane 2), $E(z)^5/E(z)^{63}$(*La*ne 3), $Thor^2$; $E(z)^5/E(z)^{63}$ (Lane 4), $Thor^{1034}$; $E(z)^5/E(z)^{63}$ (Lane 5), $E(z)^{731}/E(z)^{63}$ (Lane 6), $Thor^{1034}$; $E(z)^{731}/E(z)^{63}$ (Lane 7), $E(z)^{731}/E(z)^5$ (*Lane* 8), $Thor^2$; $E(z)^{731}/E(z)^5$(*Lane* 9), and $Thor^{1034}$; $E(z)^{731}/E(z)^5$ (Lane 10). An asterisk is noted if there is a significant difference (T-test) between the

E(z) heteroallelic mutant discs and the double *Thor; E(z)* mutant equivalent genotype discs ($P < 0.05$). Each genotype was significantly different from OR except $Thor^2$. (E) Wing discs of each genotypes were stained with phalloidin to visualize the cell membrane. Error bars represent standard error of the mean. The area of wing disc cells is used as a proxy for cell volume. An asterisk represents a statistically significant difference (T-test) *from E(z)/E(z)* ($P < 0.0001$). Each genotype was significantly different from OR.

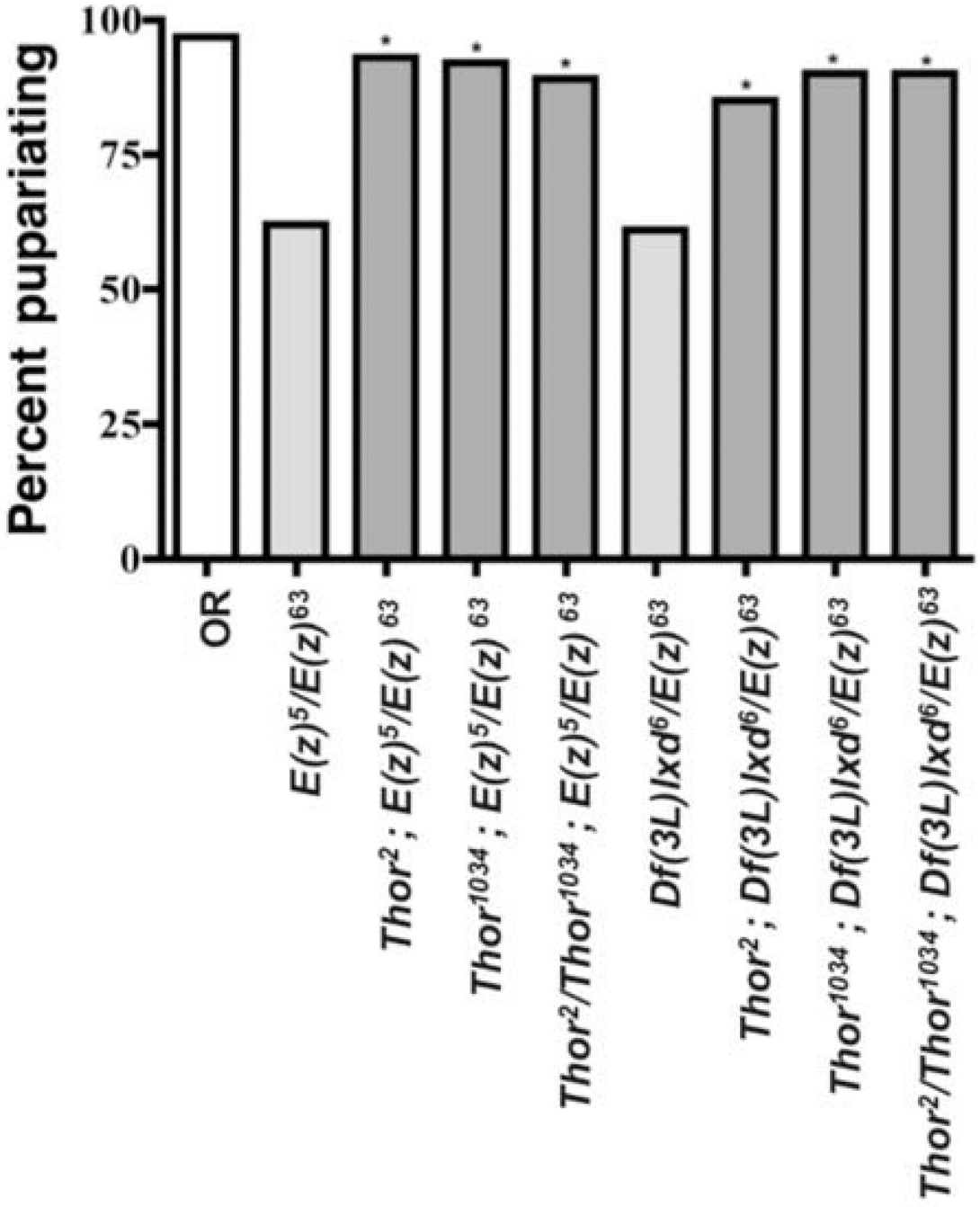

Fig. 6. Elimination of *Thor* in *E(z)* mutants increases the percent that pupariate

E(z) mutants were crossed to *Thor* mutants to generate *Thor; E(z)/TM6B* double homozygotes. These genotypes were then crossed together and progeny were scored for lethality. Over one hundred third instar larvae of each genotype were collected and scored every 24 hours to determine the fraction that formed a puparium. The graph shows the percent of third instar larvae of each genotype that formed a puparium. The *Thor; E(z)* double mutants pupariate at a significantly higher frequency than the *E(z)* mutants (Chi-square test, P<0.0001).

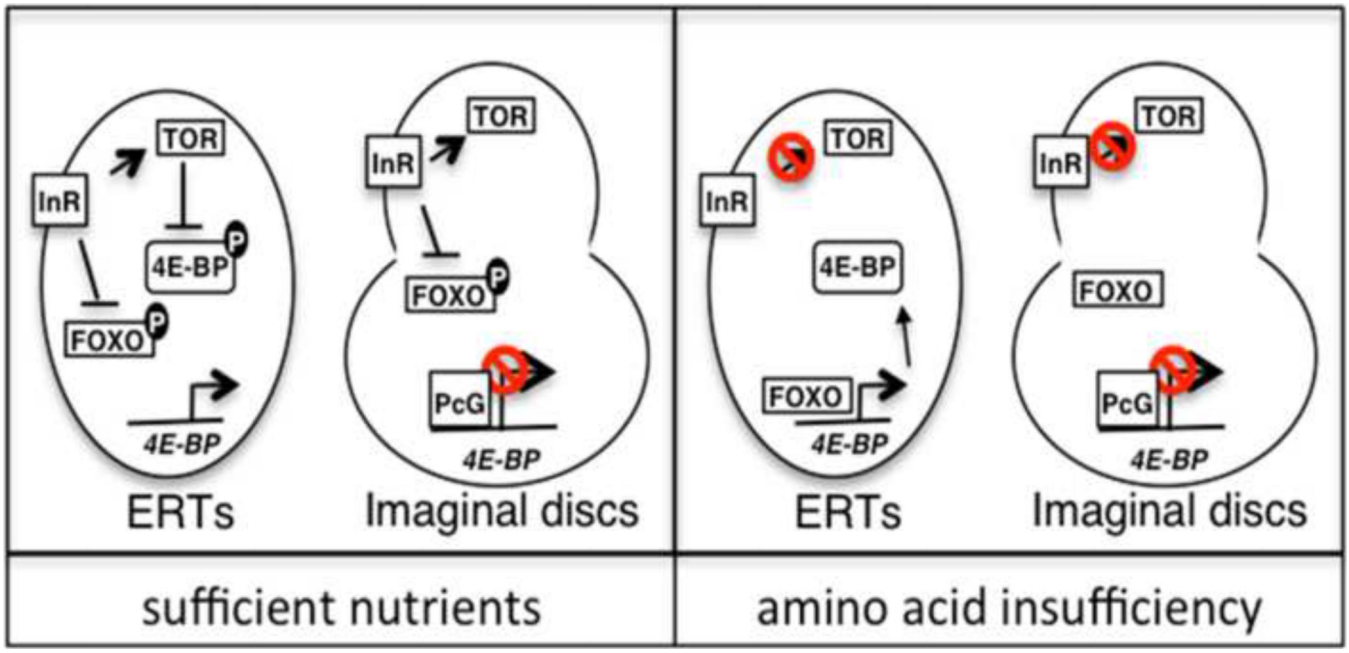

Fig. 7. Model for nutritional regulation of growth in ERTs and imaginal discs

Under conditions of sufficient nutrients, the insulin signaling and TOR signaling pathway are active in all endoreduplicating larval tissues (ERTs) and imaginal progenitor tissues, causing rapid growth and proliferation. However under conditions of amino acid insufficiency, growth is inhibited in ERTs, but only slowed in imaginal discs. In amino acid deprived ERTs, this is accomplished by down regulation of the insulin and TOR signaling pathway, which results in activation (by dephosphorylation) of FOXO and 4E-BP. In ERTs, FOXO activates transcription of *Thor*, resulting in an increase in active 4E-BP protein levels and inhibition of cell growth. However in imaginal discs, Polycomb silencing of *Thor* prevents transcriptional activation of *Thor* by FOXO and renders discs refractory to rapid cell growth arrest in response to reduced insulin and TOR signaling pathways when nutrients are insufficient. The absence of 4E-BP protein in imaginal discs allows for continue proliferating under conditions of nutrient insufficiency, possibly by utilizing energy stores in ERTs until they are depleted, which delays the onset of growth arrest of imaginal progenitors.

Table 1

jPREdictor scores for *Thor* gene orthologs in divergent *Drosophila* species

***Dros* species**	**highest jPREdictor peak**	**E value 0.05**
mel	82	55
sim	79	55
sec	75	53
yak	200	53
ere	20	55
pseudo	10	48
per	11	51
mjo	15	35
wil	54	35
vir	59	48
grim	67	36

The highest jPREdictor score is shown for each *Drosophila* species. The jPREdictor score for the E-value of 0.05 is shown for each sequence. Bold text indicates a significant jPREdictor score.